May 2006

P159 is a proteolytically processed, surface adhesin of Mycoplasma hyopneumoniae: defined domains of P159 bind heparin and promote adherence to eukaryote cells.

T. A. Burnett
University of Wollongong, tburnett@uow.edu.au

K. Dinkla
German National Centre for Biotechnology, Germany

M. Rohde
German National Centre for Biotechnology, Germany

G. S. Chhatwal
German National Centre for Biotechnology, Germany

C. Uphoff
DSMZ German Collection for Microorganisms and Cell Cultures, Germany

See next page for additional authors

P159 is a proteolytically processed, surface adhesin of Mycoplasma hyopneumoniae: defined domains of P159 bind heparin and promote adherence to eukaryote cells.

Abstract

Mycoplasma hyopneumoniae, the causative agent of porcine enzootic pneumonia, colonises the respiratory cilia of affected swine causing significant economic losses to swine production worldwide. Heparin is known to inhibit adherence of M. hyopneumoniae to porcine epithelial cilia. M. hyopneumoniae cells bind heparin but the identity of the heparin-binding proteins is limited. Proteomic analysis of M. hyopneumoniae lysates identified 27 kDa (P27), 110 kDa (P110) and 52 kDa (P52) proteins representing different regions of a 159 kDa (P159) protein derived from mhp494. These cleavage fragments were surface located and present at all growth stages. Following purification of 4 recombinant proteins spanning P159 (F1P159, F2P159, F3P159, and F4P159), only F3P159 and F4P159 bound heparin in a dose-dependent manner (Kd values 142.37 + 22.01 nM; 75.37 + 7.34 nM respectively). Scanning electron microscopic studies showed M. hyopneumoniae bound intimately to porcine kidney epithelial-like cells (PK15 cells) but these processes were inhibited by excess heparin and F4P159. Similarly, latex beads coated with F2P159 and F4P159 adhered to and entered PK15 cells, but heparin, F2P159, and F4P159 was inhibitory. These findings indicate that P159 is a post-translationally cleaved, glycosaminoglycan-binding adhesin of M. hyopneumoniae.

Keywords

Mycoplasma, hyopneumoniae, heparin

Publication Details

This article was originally published as Burnett, TA, Dinkla, K, Rohde, GS et al, P159 is a proteolytically processed, surface adhesin of Mycoplasma hyopneumoniae: defined domains of P159 bind heparin and promote adherence to eukaryote cells, Molecular Microbiology 60(3), 2006, 669-686.

Authors

T. A. Burnett, K. Dinkla, M. Rohde, G. S. Chhatwal, C. Uphoff, M. Srivasta, S. J. Cordwell, S. Geary, X. Liao, F. C. Minion, Mark J. Walker, and S. P. Djordjevic

P159 is a proteolytically processed, surface adhesin of *Mycoplasma hyopneumoniae*: defined domains of P159 bind heparin and promote adherence to eukaryote cells

Tracey A. Burnett[1,2], Katrin Dinkla[3], Manfred Rohde[3], Gursharan S. Chhatwal[3], Cord Uphoff[4], Mukesh Srivastava[1], Stuart J. Cordwell[5], Steven Geary[6], Xiaofen Liao[6], F. Chris Minion[7], Mark J. Walker[2] and Steven P. Djordjevic[1,*].

[1]NSW Department of Primary Industries, Elizabeth Macarthur Agricultural Institute, Camden, NSW 2570, Australia. [2]School of Biological Sciences, University of Wollongong, Wollongong, NSW 2522, Australia. [3]Department of Microbial Pathogenesis and Vaccine Research, GBF German Research Centre for Biotechnology, 38124 Braunschweig, Germany. [4]Department of Human and Animal Cell Lines, DSMZ German Collection for Microorganisms and Cell Cultures, 38124 Braunschweig, Germany. [5]Department of Molecular & Microbial Biosciences, University of Sydney, NSW 2006, Australia. [6]Centre of Excellence for Vaccine Research, University of Connecticut, Storrs, CT 06269-3089, USA. [7]Department of Veterinary Microbiology and Preventive Medicine, Iowa State University, Ames, Iowa 50011 USA.

*For correspondence. E-mail steve.djordjevic@dpi.nsw.gov.au; Tel. (+61) 2 46406426; Fax (+61) 2 46406384.

Summary

Mycoplasma hyopneumoniae, the causative agent of porcine enzootic pneumonia, colonises the respiratory cilia of affected swine causing significant economic losses to swine production worldwide. Heparin is known to inhibit adherence of *M. hyopneumoniae* to porcine epithelial cilia. *M. hyopneumoniae* cells bind heparin but the identity of the heparin-binding proteins is limited. Proteomic analysis of *M. hyopneumoniae* lysates identified 27 kDa (P27), 110 kDa (P110) and 52 kDa (P52) proteins representing different regions of a 159 kDa (P159) protein derived from mhp494. These cleavage fragments were surface located and present at all growth stages. Following purification of 4 recombinant proteins spanning P159 ($F1_{P159}$, $F2_{P159}$, $F3_{P159}$, and $F4_{P159}$), only $F3_{P159}$ and $F4_{P159}$ bound heparin in a dose-dependent manner (Kd values 142.37 $\pm$ 22.01 nM; 75.37 $\pm$ 7.34 nM respectively). Scanning electron microscopic studies showed *M. hyopneumoniae* bound intimately to porcine kidney epithelial-like cells (PK15 cells) but these processes were inhibited by excess heparin and $F4_{P159}$. Similarly, latex beads coated with $F2_{P159}$ and $F4_{P159}$ adhered to and entered PK15 cells, but heparin, $F2_{P159}$, and $F4_{P159}$ was inhibitory. These findings indicate that P159 is a post-translationally cleaved, glycosaminoglycan-binding adhesin of *M. hyopneumoniae*.

Introduction

Mycoplasma hyopneumoniae, the etiological agent of enzootic pneumonia (EP), ranks as one of the most economically significant diseases affecting swine production worldwide. The initial event in colonization of the respiratory tract by *M. hyopneumoniae* is binding to respiratory cilia (Blanchard *et al.*, 1992; Mebus and Underdahl, 1977; Tajima and Yagihashi, 1982). Colonisation disrupts the mucociliary escalator through ciliostasis, loss of cilia, and epithelial cell death (DeBey and Ross, 1994). Acute inflammation of airways surrounding the site of infection leads to epithelial hyperplasia and infiltration of the lamina propria by inflammatory cells composed largely of neutrophils and mononuclear cells (Livingston *et al.*, 1972). Disease resolution occurs only after a prolonged period (if at all) and once infected, swine remain recalcitrant to reinfection (Kobisch *et al.*, 1993). Most cases of EP are chronic, and are often complicated by secondary bacterial infections which exacerbate morbidity and mortality (Ciprian *et al.*, 1988). *M. hyopneumoniae* also plays a major role in the porcine respiratory disease complex in countries where infections with porcine respiratory and reproductive syndrome virus complicate respiratory disease pathology (Thacker *et al.*, 2000). Collectively, these observations indicate that losses in swine production due to this pathogen are likely to be considerably underestimated.

Genome sequence information for several strains of *M. hyopneumoniae* has facilitated proteomic studies and provided insight into families of molecules likely to play a role in the disease process (Djordjevic *et al.*, 2004; Minion *et al.*, 2004; Vasconcelos *et al.*, 2005). These advances are significant given that overall poor growth on agar surfaces coupled with a lack of development of genetic tools to selectively mutate target genes has for many years hampered efforts to identify molecules that play fundamental roles in pathogenesis (Minion, 2002). The cilium adhesin, P97 is the only cell surface adhesin that has been extensively characterized in *M. hyopneumoniae* (Hsu and Minion, 1998; Minion *et al.*, 2000). P97 is

extensively cleaved post-translationally during growth *in vitro* and processing is strain-specific. Most cleavage products remain associated with the *M. hyopneumoniae* cell surface despite the absence of hydrophobic domains or other motifs that might act to anchor these fragments to the cell membrane (Djordjevic *et al.*, 2004). Protein-protein interactions either with other *M. hyopneumoniae* proteins and/or with host-derived molecules may facilitate the localization of these cleavage fragments to the cell surface (Djordjevic *et al.*, 2004). The *p97* gene (mhp183) forms part of a two gene operon with *p102* (mhp182) (Adams *et al.*, 2005; Hsu and Minion, 1998). The *M. hyopneumoniae* genome contains six paralogs of *p97* and six of *p102* (Minion *et al*., 2004) many of which occur as two-gene operons containing a *p97* and *p102* paralog (Adams *et al.*, 2005).

Attachment of *M. hyopneumoniae* to respiratory cilia is a necessary prerequisite for epithelial damage (DeBey and Ross, 1994). Monoclonal antibodies F1B6 and F2G5, which recognise the R1 cilium binding region in P97 (Zhang *et al*., 1995), are able to reduce adherence of *M. hyopneumoniae* to respiratory cilia by approximately 70%. Purified recombinant P97 inhibits adherence of *M. hyopneumoniae* cells to cilia in a dose-dependent manner (Zhang *et al*., 1995) and binding of recombinant P97 to porcine respiratory cilia is inhibited by sulfated glycosaminoglycans (Hsu *et al.*, 1997). Consistent with these observations, P97 was recently shown to possess two heparin-binding domains (Jenkins *et al.*, 2006). Heparin, dextran sulfate, chondroitin sulfate, laminin, mucin and fucoidan also inhibit the ability of *M. hyopneumoniae* to bind respiratory cilia (Zhang *et al.*, 1994). The ability to bind glycosaminoglycans is likely to arm *M. hyopneumoniae* with the capability to bind a variety of important host molecules (Duensing *et al.*, 1999; Menozzi *et al.*, 2002; Patti *et al.*, 1994; Wadstrom and Ljungh, 1999) that also possess glycosaminoglycan binding capabilities, and thus circumvents the need to evolve specific receptors that target these molecules (Jenkins *et al.*, 2006). Although these experiments indicate that heparin-binding surface proteins are likely to be important in

pathogenesis, knowledge of heparin-binding surface proteins (apart from P97) of *M. hyopneumoniae* is lacking.

The observation that P97 is extensively modified by proteolytic cleavage suggests that other molecules secreted to the surface of *M. hyopneumoniae* may also be modified in a similar fashion. In this study we characterize a gene known as mhp494 (Minion *et al.*, 2004) that encodes a protein with a putative mass of 159 kDa (P159). We show that P159 undergoes post-translational proteolytic cleavage, generating a complex pattern of fragments that reside on the surface of *M. hyopneumoniae*. We examined the ability of *M. hyopneumoniae* cells to bind heparin and used a porcine epithelial-like cell line (PK15 cells) previously shown to bind *M. hyopneumoniae* (Zielinski *et al.*, 1990) to develop a assay to identify new adhesins and study pathogen adherence to these cells. We show that *M. hyopneumoniae* binds intimately to PK15 cells and that this ability is inhibited by pre-incubating *M. hyopneumoniae* with heparin. To understand the role that cleavage fragments of P159 play in binding heparin and adhering to PK15 cells, latex beads coated with recombinant fragments spanning different regions of this molecule were constructed and examined in our assay. Our findings indicate that P159 is a novel glycosaminoglycan binding adhesin of *M. hyopneumoniae* and that regions within P159 play a role in adherence to PK15 cells.

Results

Expression pattern of P159 in M. hyopneumoniae *strain 232*

The deduced amino acid sequence of *p159* (GenBank accession number AAV27918, mhp494) comprised 1410 amino acids with a predicted pI of 8.42. *p159* is a novel gene and its location in the genome is unusual in that it forms part of two gene structure with a *p97* paralog identified here as *p216* (mhp493; Minion *et al.*, 2004). An ongoing comprehensive peptide mass mapping study of *M. hyopneumoniae* has resolved three groups of protein spots (see boxed regions in Fig.

1A) with apparent molecular masses of 27 (P27), 52 (P52) and 110 (P110) kDa that represented different regions spanning P159. To confirm the identity of the P159 fragments, 2-D immunoblots of whole cell lysates of *M. hyopneumoniae* probed with a pool of antisera raised to recombinant fragments $F1_{P159}$-$F4_{P159}$ spanning P159 (see fig. 1C) identified P159 fragments shown in Fig. 1 (data not shown). TMpred analysis (www.ch.embnet.org/software/TMPRED_form.html) of P159 identified a single, putative transmembrane region (score 2150) between amino acids 9-29 (Fig. 1B). N-terminal sequence analysis of P27 identified a peptide sequence corresponding to the first 7 amino acids (MKKQIRN) of P159. Assuming P159 is a surface antigen (see later), this data suggests that the transmembrane domain is not removed when the P159 preprotein is secreted to the cell surface.

Based on peptide mass mapping and N-terminal sequence analyses, P27 (observed pI ~10) spans between amino acids 1-219 of the P159 sequence and cleavage at amino acid 220 would generate a protein fragment with a predicted mass of 24.5 kDa and a pI of 9.12 (Fig. 1B). Peptide mass matches of protein spots representing P52 and P110 spanned amino acids 978-1387 and 303-841 respectively (Fig. 1B) indicating that a cleavage event occurred between amino acids 220-302 and between amino acids 842-977. To generate the P110 fragment, cleavage events at amino acids 220 and 977 would generate a protein with a mass of 84.8 kDa (pI of 6.28); cleavage at amino acids 303 and 841 would generate a peptide of 60.5 kDa (pI of 8.81). Protein spots representing P110 migrate with a pI between 6-6.5 suggesting that two cleavage events probably occurred near amino acids 220 and 977. In either case, P110 has a predicted mass ranging between 61 and 85 kDa indicating that this protein fragment migrates aberrantly during SDS-PAGE. Amino acids 736-977 representing the predicted C-terminal region of P110 are enriched in acidic residues (predicted pI of 5.01) and P159 fragments such as P110 that span this region are expected to migrate with a more acidic pI compared to P27 and P52 (pI 8.85). The presence of this region in P110 is likely to contribute to its aberrant migration

during SDS-PAGE. Assuming the first cleavage scenario is correct, P52 would span amino acids 977-1410 generating a protein with a predicted mass of 49 kDa. This is largely consistent with the size and pI of P52 shown in Fig. 1A. Attempts to generate N-terminal sequence by Edman degradation for P110 and P52 cleavage fragments were unsuccessful. Collectively, these data suggest that P159 is rapidly processed during secretion to the cell surface (see later).

Purification and western blot analysis of P159 fragments

To examine the function(s) of regions within P159, four non-overlapping regions spanning the entire molecule (Fig. 1C) were cloned and expressed as poly-histidine fusion proteins in *Escherichia coli*: $F1_{P159}$, $F2_{P159}$, $F3_{P159}$, and $F4_{P159}$ comprising amino acids 31-264, 265-519 558-909 and 958-1405, respectively. $F1_{P159}$-$F4_{P159}$ were readily expressed and purified by Nickel-NTA agarose affinity chromatography (Fig. 2, panels A-D). The central region of P159 representing P110 and spanning amino acids 265-909 was cloned as two separate fragments ($F2_{P159}$ and $F3_{P159}$) because previous experience of cloning large mollicute genes in *Escherichia coli* typically resulted in an extremely poor protein yield and/or multiple translation products presumably due to the high A+T content of mycoplasmal genes (Notarnicola *et al.*, 1990). Attempts to clone and express the entire *p159* gene into *E. coli* were unsuccessful.

Rabbit antisera raised separately to purified recombinant fragments $F1_{P159}$-$F4_{P159}$ (Fig. 1C) were used to further investigate the post-translational cleavage pattern of P159 and to determine their cellular location. Antiserum raised against $F1_{P159}$ (which spans P27) reacted strongly with purified recombinant $F1_{P159}$ (Fig. 2, panel A lane 2) but reacted poorly with P27 in cell lysates of *M. hyopneumoniae* (Fig. 2, panel A, lane 1). Although the poly-histidine tag engineered into the N-terminus will contribute to the increased size of $F1_{P159}$ compared to P27, it is unlikely to account for the 4 kDa difference in apparent mass of these two proteins. Of note, the N-terminal 22-kDa cleavage fragment of the cilium adhesin P97 was also not easily detected

by immunoblotting (Djordjevic *et al.*, 2004). These data suggest that small cleavage fragments containing intact transmembrane domains may bind poorly to PVDF membrane. As expected both $F2_{P159}$ and $F3_{P159}$ antisera (which span P110) identified P110 (Fig. 2, panel B and C, lane 1). However these sera also detected a second protein with a predicted mass of approximately 68 kDa (P68) which probably represents an additional cleavage product of P159 so far undetected in our proteomic analyses (see also Fig. 2 panel E). Anti-$F4_{P159}$ serum (which spans P52) reacted with a *M. hyopneumoniae* protein equivalent in size to P52 (panel D, lane 1). Interestingly, anti-$F4_{P159}$ serum also strongly recognized a higher mass protein (> 118 kDa) when reacted with an affinity purified preparation of recombinant $F4_{P159}$ (Fig. 2, panel D, lane 2). Peptide mass mapping analysis of this higher mass protein matched the C-terminal 52 kDa region of P159 indicating that this represents an SDS-PAGE-stable, multimeric form of $F4_{P159}$ (data not shown). The higher mass form of $F4_{P159}$ was also recognized by commercial anti-poly-histidine antisera further supporting this interpretation (data not shown). Whether this multimeric form of P52 plays a role in the biology of *M. hyopneumoniae* remains unknown.

To examine the immunoblot profile of P159 during different stages of growth *in vitro*, synchronised cultures of *M. hyopneumoniae* collected between 8 h (early log phase) and 72 h (late stationary phase) post-inoculation were reacted with a pool of $F1_{P159}$-$F4_{P159}$ antisera. A consistent pattern of three strongly staining fragments of masses 52, 68, and 110 kDa (representing P52, P68 and P110) were detected at all time points suggesting that P159 is processed in an identical fashion during early log (8 h), mid-log (16-28 h) and stationary phases (40-72 h) of growth *in vitro* (Fig. 2 panel E). The P159 pre-protein was not detected suggesting that it is rapidly processed. Immunoblot profiles of whole cell lysates representing different strains of *M. hyopneumoniae*, when reacted with a pool of anti $F1_{P159}$-$F4_{P159}$, showed similar yet distinct patterns suggesting that strain-specific cleavage events occur (Fig. 2F).

Trypsin sensitivity and immuno-electron microscopy analysis of P159

To determine if P159 cleavage fragments are surface accessible, freshly cultured *M. hyopneumoniae* strain 232 cells were exposed to concentrations of trypsin ranging from 0-150 μg/ml. Exposure of intact *M. hyopneumoniae* cells to trypsin concentrations from 0.1-3 μg/ml showed a gradual loss of P68 and P110; these two proteins being almost completely digested at a trypsin concentration of 10 μg/ml. P52 was the most resilient fragment and was detectable at a trypsin concentration of 10 μg/ml but completely degraded with 50 μg/ml. There was no evidence of any P159 cleavage fragment at trypsin concentrations above 50 μg/ml (Fig. 3A). The digestion kinetics shown in Fig. 3A are similar to those of the cilium adhesin fragments that are known to reside on the cell surface (Djordjevic *et al.*, 2004) indicating that processed P159 fragments are likely to also reside on the surface of *M. hyopneumoniae*. Control experiments using antisera raised against recombinant ribosomal protein L7/L12 (shown to reside in the cytosol; Burnett *et al.*, unpublished results), pyruvate dehydrogenase subunits A and D and lactate dehydrogenase (previously shown to reside in the cytosol) were resistant to trypsin concentrations up to 300 μg/ml (data not shown; Djordjevic *et al.*, 2004).

To confirm the surface location of P159 fragments, immuno-electron microscopy was conducted using $F1_{P159}$-$F4_{P159}$ antisera. $F2_{P159}$ and $F4_{P159}$ antisera clearly showed that P159 fragments P110 and/or P68 and P52 recognized by these antisera reside on the surface of *M. hyopneumoniae* strain 232 (Fig. 3C and 3E). Control sera collected prior to immunisation with recombinant fragments reacted poorly with *M. hyopneumoniae* cells (Fig. 3B and 3D). We were unable to generate reliable images using antisera raised against $F1_{P159}$ and $F3_{P159}$ proteins because of unacceptable levels of gold labeling with preimmune sera (data not shown).

213 M. hyopneumoniae *binds heparin*

214 Various glycosaminoglycans have been shown to interfere with the ability of ***M. hyopneumoniae***
215 to adhere to porcine cilia (Zhang ***et al.***, 1994). Fig 4A shows that biotinylated heparin binds to
216 the surface of freshly cultured cells of ***M. hyopneumoniae*** strain 232 in a dose dependent and
217 saturable manner. ***M. hyopneumoniae*** strain 232 proteins ranging in mass from 15 to 150 kDa
218 bind biotinylated heparin (Fig. 4B).

219

220 *Domains within P159 bind heparin*

221 With the aim of determining the function(s) of P159 and specifically determine if any of its
222 cleavage fragments bind heparin, a panel of extracellular matrix (ECM) components (including
223 fibronectin, laminin, collagen and fibrinogen) and various glycosaminoglycans (including
224 heparin, heparan sulfate, mucin, chondrotin sulfate A and B and fucoidan), were tested for either
225 their ability to bind directly to recombinant fragments of P159, or to interfere with binding to
226 one of these components. Although none of the recombinant fragments bound any of the ECM
227 proteins, $F3_{P159}$ and $F4_{P159}$ bound biotinylated heparin in a saturable and dose-dependent manner
228 with saturation occurring between 15-20 μg/ml (0.5-1.5 μM) of biotinylated heparin. A 50-fold
229 excess of unlabelled heparin was found to extinguish > 90% of the signal (Fig. 5) indicating that
230 heparin occupies specific binding sites on both F3 and F4. Non-linear regression and one-site
231 binding analyses were performed on the specific binding data producing an estimate of the
232 apparent dissociation constants for $F3_{P159}$- and $F4_{P159}$- biotinylated heparin complexes of 142.37
233 $\pm$ 22.01 nM (2.13 $\pm$ 0.44 μg/ml) and 75.37 $\pm$ 7.34 nM (1.13 $\pm$ 0.11 μg/ml) respectively. To
234 further investigate the interaction of F3 and F4 with heparin, binding of these proteins to a
235 heparin-agarose (Sigma-Aldrich, St. Louis, Missouri) column was investigated. Both $F3_{P159}$ and
236 $F4_{P159}$ bound to the heparin-agarose column and were eluted with 10 mM Tris containing
237 approximately 0.22 M NaCl and 0.32 M NaCl respectively (data not shown).

238 The kinetics of binding biotinylated heparin by $F3_{P159}$ and $F4_{P159}$ was examined in more
239 detail. At concentrations between 1-250 μg/ml, heparin profoundly affected the ability of $F3_{P159}$
240 and $F4_{P159}$ to bind biotinylated heparin with concentrations > 500 μg/ml effectively blocking
241 binding (Fig. 6A). Non-linear regression with one-site competition determined the 50%
242 inhibitory concentration (IC_{50}) for $F3_{P159}$ and $F4_{P159}$ to be 52.92 $\pm$ 1.03 μg/ml and 66.63 $\pm$ 1.02
243 μg/ml, respectively. Various glycosaminoglycans were tested for their ability to inhibit the
244 binding of $F3_{P159}$ and $F4_{P159}$ to biotinylated heparin (Fig. 6B and C). Fucoidan, a highly sulfated
245 fucose polymer, effectively inhibited the binding of both $F3_{P159}$ and $F4_{P159}$ to biotinylated
246 heparin with IC_{50} values of 96.28 $\pm$ 1.19 μg/ml and 36.23 $\pm$ 1.14 μg/ml, respectively. Heparan
247 sulfate, chondroitin sulfate A, chondroitin sulfate B (Fig. 6), and mucin (results not shown) were
248 unable to inhibit the binding of $F3_{P159}$ or $F4_{P159}$ to biotinylated heparin.
249
250 *Adherence and invasion of PK15 cell monolayers by* M. hyopneumoniae**.**
251 Radiolabelled *M. hyopneumoniae* strains J, 232 and 144L have previously been shown to adhere
252 to a porcine kidney epithelial-like (PK15) cell line in a receptor-dependent manner and their
253 adherence was blocked by either pre-treating PK15 cells with unlabelled *M. hyopneumoniae* or
254 by pre-treating *M. hyopneumoniae* cells suspensions with trypsin (Zielinski *et al*., 1990). In our
255 study we examined the ability of *M. hyopneumoniae* strain J cells to interact with PK15 cell
256 monolayers by scanning electron microscopy. We showed that *M. hyopneumoniae* adheres
257 intimately to the surface of PK15 cells with the mycoplasma often seen closely associated with
258 microvilli on the surface of the monolayers (Fig. 7A). *M. hyopneumoniae* cells were separately
259 pre-incubated with recombinant fragments $F1_{P159}$-$F4_{P159}$ prior to addition to PK15 cells to
260 determine if regions within P159 influence the ability of mycoplasma cells to bind to the
261 monolayers. When *M. hyopneumoniae* cells were pre-incubated with 1 μg of $F4_{P159}$ protein [and
262 not $F1_{P159}$, $F2_{P159}$ or $F3_{P159}$, (data not shown)], an obvious decrease in adherence was observed

263 (Fig. 7B). *M. hyopneumoniae* cells pre-incubated with a saturating concentration of heparin (500
264 μg/ml) also bound poorly to the surface of PK15 cell monolayers (Fig. 7C). Purified
265 immunoglobulins (25 μg) from serum obtained from rabbits separately immunized with $F1_{P159}$,
266 $F2_{P159}$, $F3_{P159}$ and $F4_{P159}$ proteins did not appear to affect the ability of *M. hyopneumoniae* to
267 adhere to PK15 cells or the uptake and entry of latex beads (see later) coated with P159
268 recombinant fragments (data not shown).
269 To define domains within P159 that might play a role in adherence to PK15 cells, a latex
270 bead binding assay was used. Adherence was observed by a combination of double-
271 immunofluorescence microscopy (Fig. 8) and scanning electron microscopy (Fig. 9). Latex
272 beads separately coated with $F2_{P159}$, $F3_{P159}$ and $F4_{P159}$ were found to adhere to PK15 cells within
273 2 h incubation at 37˚C (Fig. 8). Furthermore, latex beads coated with $F2_{P159}$ and $F4_{P159}$ (but not
274 $F1_{P159}$ or $F3_{P159}$) were detected inside PK15 cells (Fig. 8 see arrows) between 2-22 h post-
275 incubation and increasing numbers of internalized beads were detected over this time (results not
276 shown). Latex beads alone (data not shown) or beads coated with recombinant $F1_{P159}$ protein
277 (Fig. 8A) did not adhere to or enter PK15 cells.
278 To examine the specificity of binding of $F1_{P159}$ - $F4_{P159}$ - coated latex beads to PK15
279 cells, binding experiments using latex beads that had been separately pre-incubated with
280 recombinant P159 fragments (1 μg each) were performed and examined by scanning electron
281 microscopy. In preliminary experiments, pre-incubation with soluble $F2_{P159}$, $F3_{P159}$ and $F4_{P159}$
282 reproducibly decreased the attachment of $F2_{P159}$ - (Fig. 10A), $F3_{P159}$ - (data not shown) and
283 $F4_{P159}$ - (Fig. 10B) coated latex beads to PK15 cells. Similarly, when $F4_{P159}$-coated latex beads
284 were pre-incubated with heparin they poorly bound to PK15 cell monolayers (Fig. 10C and D).
285 The effect of pre-incubating $F2_{P159}$ - and $F4_{P159}$ - coated latex beads separately with heparin and
286 with excess $F2_{P159}$ and $F4_{P159}$ proteins on their ability to adhere to and enter PK15 cells is
287 summarized in Fig. 10D. Pre-incubation of $F2_{P159}$ - and $F4_{P159}$ - coated latex beads with a

saturating concentration of heparin inhibited binding to PK15 cells by 89 and 64% respectively (Fig. 10D). Significantly, heparin completely abolished entry of $F2_{P159}$ - and $F4_{P159}$ - coated latex beads into PK15 cells (Fig. 10D). Pre-incubation of $F4_{P159}$- coated latex beads with excess $F4_{P159}$ inhibited the binding and entry of $F4_{P159}$ - coated latex beads by 71% and 67% respectively and displayed the greatest ability of all the P159 recombinant proteins to inhibit the binding and invasion of latex beads coated with recombinant P159 proteins (Fig. 10D).

Discussion

mhp494 encodes a protein with a predicted mass of 159 kDa (P159) and is unusual in that it forms part of a two gene structure with mhp493, a putative cilium adhesin paralog (Minion *et al.*, 2004). MALDI-TOF mass spectrometric analyses of *M. hyopneumoniae* proteins separated by 2-D gel electrophoresis identified proteins with masses of 27, 52 and 110 kDa that represented regions within P159. Immunoblotting studies using monospecific antisera raised to different regions of mhp494 readily identified these and other proteins (putative cleavage fragments) with masses between 27-110 kDa in whole cell lysates of *M. hyopneumoniae* harvested during early, mid, late exponential and stationary phases of growth indicating that P159 is extensively cleaved post-translationally. A high mass protein that might represent P159 was virtually undetectable by immunoblotting indicating that P159 is rapidly processed, probably by a proteolytic enzyme(s). Trypsin digestion studies confirmed that the majority of these cleavage fragments reside on the cell surface despite the absence of hydrophobic stretches of amino acids that might anchor these peptides to the cell membrane. The N-terminal sequence MKKQIRN (amino acids 1-7 in Mhp494) obtained from the N-terminal cleavage fragment P27 precedes the only significant transmembrane domain in P159 (amino acids 9-29; TMpred score 2150) consistent with a hypothesis that cleavage occurs simultaneously with or immediately after translation and secretion to the cell surface.

These observations bear a striking resemblance to those reported for the cilium adhesin P97 (mhp183); i) the P126 pre-protein is barely detectable by immunoblot and is extensively cleaved, generating fragments ranging in mass from 20-120 kDa (Djordjevic *et al.*, 2004), ii) the N-terminal cleavage fragment P22 contains the only significant transmembrane domain found in the molecule, yet many of the cilium adhesin cleavage fragments are present on the cell surface and iii) processing is strain-specific. These observations suggest that P159 and P126 pre-proteins are processed via the same pathway. Although the surface topography of *M. hyopneumoniae* is poorly understood we have now provided evidence that three high-mass surface proteins of *M. hyopneumoniae* P159 (this study; mhp494), P97 (mhp183) and P102 (mhp182) (Djordjevic *et al.*, 2004) are cleaved with fragments residing on the cell surface. No evidence for proteolytic processing was reported for two well characterized surface lipoproteins with masses of 65 kDa (Kim *et al.*, 1990) and 46 kDa (Futo *et al.*, 1995). These data suggest that surface molecules secreted via type II but not type I secretory pathways may be targeted for further proteolytic processing in *M. hyopneumoniae* but additional studies are needed to rigorously test this hypothesis. The identity and specificity of the corresponding protease(s) that cleave these proteins remains unknown. However, bioinformatic analysis of the *M. hyopneumoniae* genome identified five proteins with aminopeptidase signatures (mhp209, Map; mhp462, PepA; mhp520, PepF; mhp680, PepP; and mhp656, Gcp) and a further two with serine protease signatures (mhp287 and mhp292). One or several of these are suspected of playing a role in surface protein processing.

BlastP analyses showed that mhp494 is a novel molecule with discrete regions showing limited homology to proteins found in *Mycoplasma conjunctivae* and *M. hyopneumoniae*. Specifically, two regions spanning amino acids 1004-1406 and 2-200 of P159 showed 22% identity (41% similarity) and 25% identity (46% similarity) respectively with LppT from *Mycoplasma conjunctivae* (Belloy *et al.*, 2003). *lppT* is the second gene in a two-gene operon

with *lppS* which was reported to be an adhesin in this species (Belloy *et al.*, 2003). Furthermore, amino acids 1026-1165 displayed 26% identity (48% similarity) with mhp182 (P102) and amino acids 10-209 and 17-191 showed 28% identity (51% similarity) and 28% identity (44% similarity) with P102 paralogs mhp272 and mhp384 respectively.

Different strains of *M. hyopneumoniae* have been shown to adhere to PK15 cell monolayers (Zielinski *et al.*, 1990) but in that study adherence was monitored by counting radiation emitted from radiolabelled adhering cells. Scanning electron microscopy studies reported here show that *M. hyopneumoniae* strain J adheres intimately to PK15 cells especially in regions where microvilli are prominent. Pre-incubating *M. hyopneumoniae* cells with a saturating concentration of heparin almost completely abolished binding to PK15 cells, underscoring the importance that heparin binding proteins on the surface of *M. hyopneumoniae* play in adherence to eukaryote cells. Importantly, Zhang *et al.* (1994) showed that heparin significantly inhibited the ability of *M. hyopneumoniae* to adhere to preparations of porcine respiratory tract cilia. Collectively, these studies indicate that PK15 cell monolayers provide a useful model system for identifying adhesins in *M. hyopneumoniae*. To this end we showed that P159 recombinant fragments $F2_{P159}$ and $F4_{P159}$ (and to a limited extent $F3_{P159}$) which span all but the N-terminal 27 kDa of P159 promote the ability of latex beads to bind to PK15 cells demonstrating that P159 is a novel eukaryote cell adhesin. Pre-incubation of $F2_{P159}$– and $F4_{P159}$–coated latex beads with a saturating concentration of heparin significantly blocked the ability of these beads to adhere to, and completely abolished their entry into, PK15 cells.

Recombinant fragments $F3_{P159}$ and $F4_{P159}$, which span the C-terminal half of P159, were found to bind heparin in a dose-dependent, saturable and specific manner (Kd values of 142.37 $\pm$ 22.01 nM and 75.37 $\pm$ 7.34 nM respectively). $F3_{P159}$ and $F4_{P159}$ were also shown to bind to heparin-agarose showing that these P159 recombinant fragments bind both soluble and bound heparin. These values are comparable to other biologically significant heparin-protein binding

363 interactions (Pethe *et al*., 2000) and fall in the midrange of other reported constants for heparin-
364 protein interactions (Pankhurst *et al.*, 1998). The ability of $F2_{P159}$ to promote the adherence of
365 latex beads to PK15 cells despite an inability to bind heparin suggests that different regions
366 within P159 use different mechanisms to bind eukaryote cells. Our data suggests that P159
367 cleavage fragments P110 and P52 each possess the ability to bind heparin and to adhere to PK15
368 cells; the function of $F1_{P159}$ remains unknown. *M. hyopneumoniae* cells pre-incubated with an
369 excess of $F4_{P159}$ protein were significantly affected in their ability to adhere to PK15 cells
370 suggesting that the C-terminal region of P159 spanning P52 interacts with a receptor(s) on the
371 surface of PK15 cells. Further processing events that affect the integrity of P110 and P52 may
372 have important ramifications for their biological function. Immunoblotting studies (Fig. 2)
373 indicate that P68 resides within P110 and further studies are needed to examine the biological
374 properties specific to this fragment.
375 It is becoming evident from this and previous studies (Djordjevic *et al.*, 2004; Jenkins *et*
376 *al*., 2006) that *M. hyopneumoniae* processes key surface proteins to generate domains with
377 potentially important biological functions. Processing of surface proteins may provide *M.*
378 *hyopneumoniae* with a means to regulate its surface architecture enabling it to adapt to various
379 tissue environments within the host. Cytokines, growth factors, complement components, plasma
380 lipoproteins, regulators of homeostasis, and various extracellular matrix components such as
381 vitronectin and fibronectin have been shown to bind heparin (Bernfield *et al.*, 1999; Jackson *et*
382 *al*., 1991; Kim *et al.*, 1990). Microbial pathogens bind heparin and related glycosaminoglycans
383 as a means of recruiting a wide variety of mammalian heparin binding proteins to their surface,
384 thus bypassing the need to evolve specific receptor molecules for these key mammalian proteins
385 (Duensing *et al.*, 1999). More importantly, the ability to recruit these proteins to the surface of
386 microbial pathogens impacts on key aspects of microbial pathogenicity such as an increased

capacity to invade epithelial cells and inhibition of chemokine-induced chemotaxis (Duensing *et al.*, 1999).

The ability of a protein to bind glycosaminoglycans largely depends on electrostatic interactions between the negatively charged sulfate groups and positively charged regions of the protein; the role of different sugar moieties in the backbone of the glycosaminoglycan in protein binding is less well understood. Although the heparin-binding motifs, XBBXBX and XBBBXXBX (where B represent basic amino acids and X any other amino acids) have been known for many years (Cardin and Weintraub, 1989), more recent studies indicate that various combinations of clustered basic amino acids can bind heparin (Aoki *et al.*, 2004). P159 is rich in lysine (K) and arginine (R) residues (15.6% and 13.9% of $F3_{P159}$ and $F4_{P159}$ sequences respectively are K and R), and further studies aim to more accurately delineate the heparin binding domains within regions of P159.

Fucoidan, a sulfated polysaccharide of non-mammalian origin, inhibited the interaction between heparin and $F3_{P159}$ and $F4_{P159}$. It is generally the case that heparin-binding proteins also interact with fucoidan due to its high sulfate density and branched, comb-like structure, which contrasts with the linear structure of mammalian glycosaminoglycans (Patankar *et al.*, 1993). Chondroitin sulfate A and B and mucin did not competitively inhibit the ability of heparin to bind P159 fragments $F3_{P159}$ and $F4_{P159}$; heparan sulfate, a less sulfated version of heparin, only slightly inhibited these interactions. Chondroitin sulfate B is similar in structure to heparin and heparan sulfate in that it contains a backbone of iduronate residues yet failed to act as a competitive inhibitor. Collectively, these observations suggest that the degree of sulfation is a key component in $F3_{P159}$ and $F4_{P159}$ binding heparin.

In conclusion, evidence presented here indicates that P159 is a proteolytically processed, heparin binding surface protein of *M. hyopneumoniae* and that the C-terminal half of P159 houses at least 2 heparin-binding domains located within $F3_{P159}$ and $F4_{P159}$ respectively. We

show that i) *M. hyopneumoniae* adheres intimately to the surface of PK15 cells where microvilli predominate, ii) heparin blocks the ability of this pathogen to adhere to PK15 cells and iii) regions within P159 are intimately involved in adherence to PK15 cells. Despite possessing limited coding capacity, evidence of differences in strain virulence (Vicca *et al.*, 2003), cleavage of key surface proteins (Djordjevic *et al.*, 2004), and our recent report that key surface proteins bind glycosaminoglycans (Jenkins *et al.*, 2006) suggests that subtle changes in surface protein sequences may have significant ramifications for disease caused by *M. hyopneumoniae*.

Experimental procedures

Bacterial strains and growth conditions.

M. hyopneumoniae strain 232 (Zhang *et al*., 1995) was a kind gift from F. C. Minion. Two strain J isolates were used in these studies; NCTC 10110 was used for immunoblot experiments and a low passage isolate derived from ATCC 27715 was used for infection studies of PK15 cells. The ATCC 27715 strain was kindly provided by P. Valentin-Weigand, University of Veterinary Medicine Hannover, Germany. A description of *M. hyopneumoniae* strains Beaufort, Sue and C1735/2 and their source has been described previously (Scarman *et al.*, 1997). *M. hyopneumoniae* was grown in 0.22 μm filter sterilized modified Friis broth (Friis, 1975) and harvested as described previously (Djordjevic *et al.*, 2004). For growth studies, sterile tubes containing 6 ml of Friis broth were simultaneously inoculated with 300 μl of *M. hyopneumoniae* strain 232 culture and incubated for 8, 16, 24, 28, 32, 40, 48, 56 and 72 h as described previously (Djordjevic *et al.*, 1994). *Escherichia coli* M15 [pREP4] cells (Qiagen, Alameda, California) were grown at 37^{o}C in Luria-Bertani medium (Sambrook *et al*., 1989). When appropriate, antibiotics were used at the following concentrations: ampicillin 100 μg/ml and kanamycin 25 μg/ml. Protein expression was induced by the addition of 100 μM isopropyl-β-D-thiogalactopyranosidase (IPTG).

437

438 *Proteomic analyses: 2-D gel electrophoresis and postseparation analyses.*

439 Two-dimensional gel electrophoresis (2-DGE) was carried out as described previously
440 (Cordwell *et al*., 1997). Conditions used for the solubilisation of *M. hyopneumoniae* proteins,
441 isoelectric focusing and SDS-PAGE have been described previously in detail (Djordjevic *et al.*,
442 2004). Briefly, *M. hyopneumoniae* bacterial cells were resuspended in 1 ml of sample buffer for
443 each 0.1 g of bacterial pellet. Cells were disrupted with a Microson Ultrasonic sonicator
444 (Misonix, Farmingdale, New York) for 6 x 30 sec at a power setting of 14 W and centrifuged
445 (120 min, 50 000 x g) in a Beckman TL100 ultracentrifuge (Beckman Coulter, Fullerton,
446 California). A total of 250 µg of *M. hyopneumoniae* protein extract was diluted with sample
447 buffer to a volume of 100 µl for application to the anodic end of each IPG strip in an applicator
448 cup. Isoelectric focusing was performed on a Multiphor II electrophoresis unit (Amersham
449 Biosciences, Piscataway, New Jersey) for 85 kVh at 20^{o}C. IPG strips were detergent exchanged,
450 reduced, and alkylated in buffer containing 6 M urea, 2% SDS, 20% glycerol, 5 mM tributyl
451 phosphine, 2.5% (v/v) acrylamide monomer, a trace amount of bromophenol blue dye, and 375
452 mM Tris-HCl (pH 8.8) for 20 min prior to loading the IPG strip onto the top of a 8-18% 20 cm
453 by 20 cm polyacrylamide gel. Second-dimension electrophoresis was carried out at 5^{o}C using 3
454 mA/gel for 2 h followed by 20 mA/gel until the bromophenol blue dye had run to the end of the
455 gel. Gels were fixed in 40% methanol and 10% acetic acid for 1 h, stained overnight in Sypro
456 Ruby (Molecular Probes, Eugene, Oregon) and images acquired using a Molecular Imager Fx
457 apparatus (Bio-Rad Laboratories, Hercules, California). Gels were then double stained in
458 Coomassie blue G-250. Protein spots were excised from gels using a sterile scalpel blade and
459 placed into 96-well V bottom trays (Greiner Bio-One, Longwood, Florida). The methods used
460 for post-separation analyses are as described previously (Djordjevic *et al.*, 2004). A list of
461 monoisotopic peaks corresponding to the mass of generated tryptic peptides was used to search a

462 modified translated version of the *M. hyopneumoniae* genome (Minion *et al*., 2004). N-terminal
463 Edman sequencing was performed as previously described (Nouwens *et al*., 2000).
464
465 *Molecular analyses, cloning and expression.*
466 Plasmid DNA was prepared using a plasmid MidiPreparation kit (Qiagen, Alameda, California)
467 as per manufacturer's instructions. DNA sequence analysis was performed using the Sanger
468 method. PCR was carried out using a DTCS Quickstart Master Mix (Beckman Coulter,
469 Fullerton, California), according to the manufacturer's instructions and analysed using a
470 CEQ8000 Genetic Analyser (Beckman Coulter, Fullerton, California). Both pQE-9 specific
471 primers and internal primers were used to initiate sequencing of DNA and were purchased from
472 Sigma-Aldrich (Sydney, Australia). Hexahistidyl P159 fusion proteins were constructed using
473 pPCR-Script (Stratagene, La Jolla, California) and pQE-9 (Qiagen, Alameda, California) cloning
474 vectors. Primer sequences used to amplify each of the four fragments are given in Table 1. The
475 underlined sequences correspond to the following restriction sites: *Sal*I in the forward primers
476 and *Pst*I in the reverse primers. Recombinant proteins $F1_{P159}$-$F4_{P159}$ span nucleotides 91-791
477 (amino acids 31-264), 792-1557 (amino acids 265-519), 1675-2727 (amino acids 558-909) and
478 2875-4215 (amino acids 958-1405) respectively within the *p159* gene sequence (accession
479 number AF279292). PCR was carried out using Expand DNA Polymerase Enzyme (Roche,
480 Basel, Switzerland) on a PC-960 thermocycler (Corbett Research, Mortlake, Australia). The
481 template for the amplification of the entire *p159* gene was *M. hyopneumoniae* 232. The resulting
482 4233 bp amplicon was cloned into the pCR2.1 TA plasmid (Invitrogen, Carlsbad, California).
483 The nine tryptophan-encoding TGA codons present in this ORF were converted to TGG by site-
484 directed mutagenesis using the QuikChange Site Directed Mutagensis Kit (Stratagene, La Jolla,
485 CA) according to the manufacturers suggested protocol. The resulting clone was designated
486 p110SDM c1. Amplification and site directed mutagenesis primers are indicated in Table 1. PCR

fragments were digested with *Sal*I and *Pst*I and cloned into *Sal*I and *Pst*I-digested pPCR-Script plasmid (Stratagene, La Jolla, California). Constructs with the proper fragment orientation were identified by restriction digestion and DNA sequence analysis and were designated p159PCR1-4. Regions of p159 within p159PCR1-4 were digested with *Sal*I and *Pst*I and cloned into pQE-9 (Qiagen, Alameda, California) using T4 DNA ligase (Roche, Basel, Switzerland) and transformed into *E. coli* M15 [pREP4] cells (Qiagen, Alameda, California) by electroporation using a Gene Pulsar (Bio-Rad Laboratories, Hercules, California) and the pre-set *E. coli* protocol at 2.5 kV. Correct constructs were identified as above and designated p159QE1-4. Protein expression was induced by the addition of 100 μM IPTG and proteins were purified using Ni-NTA agarose as per the manufacturer's instructions (Qiagen, Alameda, California). The presence of possible transmembrane domains was investigated using the TMPred program available via the Swiss European Molecular Biology Network (EMBnet) website (www.ch.embnet.org/software/TMPRED_form.html).

Latex bead preparation and PK15 cell culture.

As per previously published methods (Dombek *et al*., 1999; Molinari *et al*., 1997), latex beads (3 μm; Sigma-Aldrich, St. Louis, Missouri) were coated with purified recombinant P159 fragments $F1_{P159}$-$F4_{P159}$. Briefly, 10^8 bead particles in 50 μl PBS were incubated with 5 μg of purified proteins in PBS overnight at 4°C. After washing steps, free binding sites on the bead surface were blocked by incubation with 200 μl of 10 mg/ml BSA in PBS for 1 h at room temperature. The efficiency of particle loading was verified by fluorescence-activated cell sorter analysis with anti-$F1_{P159}$-$F4_{P159}$ rabbit serum (results not shown). Beads were washed and the volume adjusted to 2.5 ml with Dulbecco modified Eagle medium (Invitrogen, Karlsruhe, Germany) with HEPES and 1% foetal calf serum. PK15 cells (American type culture collection certified cell line 33) were seeded on 12-mm-diamater glass coverslips (Nunc, Wiesbaden, Germany) placed on the

512 bottom of 24-well tissue culture plates (Nunc, Wiesbaden, Germany) at 1.5 x 10^5 cells per well
513 and allowed to grow to semi-confluent monolayers at 37°C in a 5% CO_2 atmosphere. After
514 addition of 250 µl of the bead suspension, the cells were incubated for 2, 4, 7 and 22 h at 37°C in
515 a 5% CO_2 atmosphere. Cells were washed three times with PBS to remove unbound beads.
516 Cells were either processed for scanning electron microscopy (Molinari *et al*., 1997) or for
517 double immunofluorescence microscopy as described below. Further studies were conducted
518 pre-incubating the latex beads with a saturating concentration of heparin (500 µg/ml), purified
519 $F1_{P159}$, $F2_{P159}$, $F3_{P159}$, and $F4_{P159}$ proteins (1 µg each), or anti-$F1_{P159}$-$F4_{P159}$ sera (25 µg)
520 separately for 1h at 37°C in a 5% CO_2 atmosphere before addition to the PK15 cells.
521 PK15 cells were seeded on 12-mm-diamater glass coverslips placed on the bottom of 24-
522 well tissue culture plates at 1.5 x 10^5 cells per well and allowed to grow to semi-confluent
523 monolayers at 37°C in a 5% CO_2 atmosphere. A 5 ml fresh *M. hyopneumoniae* (strain J, ATCC
524 27715) culture was centrifuged at 10,000 × g and resuspended in 100 µl of Dulbecco modified
525 Eagle medium (Invitrogen, Karlsruhe, Germany) with HEPES and 1% foetal calf serum. 10 µl of
526 *M. hyopneumoniae* suspension per well was added to 0.5 ml of confluent PK15 cells and
527 incubated at 37°C in a 5% CO_2 atmosphere for 2 h. The wells were then prepared for electron
528 microscopy as reported previously (Molinari *et al*., 1997). Additional experiments where *M.*
529 *hyopneumoniae* was pre-incubated with a saturating concentration of heparin (500 µg/ml),
530 purified $F1_{P159}$, $F2_{P159}$, $F3_{P159}$, and $F4_{P159}$ proteins (1 µg each), or anti-$F1_{P159}$-$F4_{P159}$ sera (25 µg)
531 separately for 1h at 37°C in a 5% CO_2 atmosphere before addition to the PK15 cells were
532 conducted.
533
534 *Antisera, immunotechniques and microscopy.*

Antisera to each fragment of P159 were generated by subcutaneous immunization of New Zealand White rabbits with hexahistidyl-tagged products purified by nickel-affinity chromatography. Pre-immune sera were collected prior to immunization for the preparation of control serum. Rabbits were then each immunized on two occasions 21 days apart using Freund's incomplete adjuvant (Sigma-Aldrich, St. Louis, Missouri), and immune responses monitored by immunoblotting. Rabbits were euthanased, and serum collected as described previously (Wilton *et al*., 1998). Horse radish peroxidase-conjugated sheep anti-rabbit immunoglobulin antibodies were purchased commercially (Chemicon, Temecula, California).

M. hyopneumoniae whole cell protein preparations and purified hexahistidyl $F1_{P159}$-$F4_{P159}$ proteins along with *M. hyopneumoniae* growth assay samples were subjected to electrophoresis on 12% SDS-PAGE gels as described previously (Laemmli, 1970). After electrophoresis, proteins were electrophoretically transferred onto polyvinylidene difluoride membrane using a Hoefer Scientific TE Series Transphor Electrophoresis Unit (Hoefer, San Francisco, California) as described previously (Burnette, 1981). Immunoblotting experiments were performed with rabbit polyclonal antibodies raised against $F1_{P159}$-$F4_{P159}$, either separately or pooled. Peroxidase conjugated sheep anti-rabbit was used as the secondary antibody and detected using diaminobenzidine (DAB; Sigma-Aldrich, St. Louis, Missouri).

PK15 cells (after incubation with the coated latex beads) were washed with PBS and then fixed by the addition of 0.5 ml/well of pre-cooled fixation buffer (1% paraformaldehyde in PBS), the tray was placed on ice for 1 h and then stored at 4^{o}C overnight. The PK15 cells were blocked by the addition of 200 µl/well of PBS with 10% FCS and incubated for 30 min at room temperature. The blocking solution was then removed and the cells incubated separately with 200 µl/well of the anti-$F1_{P159}$-$F4_{P159}$ rabbit polyclonal antibodies (40-50 µg/ml) for 45 min at room temperature. Cells were incubated with goat anti-rabbit Alexa 488 (green) (Molecular Probes, Eugene, Oregon) for 1h at room temperature and subsequently washed with PBS. Cells

were permeabilized with Triton X-100 (200 µl/well of a 0.1% triton X-100 in PBS solution) for 5 min at room temperature, washed in PBS, followed by incubation with 200 µl/well of the anti-F1-F4 rabbit polyclonal antibodies (40-50 µg/ml) for 45 min at room temperature. After washing, cells were treated with goat anti-rabbit Alexa 568 (red) (Molecular Probes, Eugene, Oregon) for 1 h and washed three times in PBS. Some cells were further incubated with 200 µl of a 0.1 mg/ml Hoechst stain (Molecular Probes, Eugene, Oregon) solution in PBS for 5 min before being washed three times in PBS. Cells were then mounted onto a glass slide. After this labeling procedure, extracellular beads appear yellow/green whereas intracellular beads are stained orange/red. Images were recorded using a Zeiss inverted microscope 100 M with an attached Zeiss Axiocam HRc digital camera.

Immunogold labelling of whole *M. hyopneumoniae* cells was performed as follows: Parlodion/carbon coated 300 mesh nickel grids (Pro Sci Tech, Queensland, Australia) were floated on drops of *M. hyopneumoniae* (strain 232) suspension in a moist petridish for 2 min. The grids were then incubated for 1 min with phosphate buffer (pH 6.8) containing 1% BSA, 0.5% Tween 20 and 0.02% sodium azide. The grids were then floated on drops of undiluted anti-F2 and anti-F4 sera, pre-immune for control and post-immune for tests, and incubated at 37^{o}C for 90 min. The grids were washed with phosphate buffer (pH 6.8) 3 x 5 min and then floated on drops of protein A gold (15 nm, BBInternational, Cardiff, UK) diluted 1:50 for 45 min. The grids were washed with phosphate buffer and distilled water and stained with 2% aqueous uranyl acetate (Merck, Whitehouse Station, New Jersey). The grids were blotted dry and examined under a Philips 208 transmission electron microscope.

Trypsin treatment of M. hyopneumoniae

M. hyopneumoniae cells (0.5 g) were treated with trypsin as described previously (Wilton *et al.*, 1998). Briefly, trypsin was added to cell suspensions of *M. hyopneumoniae* at trypsin

585 concentrations of 0, 0.1, 0.5, 1, 3, 5, 10, 50 and 150 µg/mL and incubated at 37°C for 15 min.
586 Cell suspensions were then lysed in sample buffer (60 mM Tris, pH 6.8; 1% [w/v] SDS; 1%
587 [v/v] β-mercaptoethanol; 10% [v/v] Glycerol and 0.01% [w/v] bromophenol Blue) and heated to
588 95°C for 10 min. Lysates were analysed by SDS-PAGE and immunoblotting with a pool of
589 $F1_{P159}$-$F4_{P159}$ antiserum.
590
591 *Heparin binding assays.*
592 Paraformaldehyde (1% paraformaldehyde in PBS) fixed *M. hyopneumoniae* strain 232 cells at an
593 optical density of 0.04 (in 0.1 M $NaHCO_3$, pH 9.5) or aliquots (100 µl) of recombinant proteins
594 $F1_{P159}$-$F4_{P159}$ (5 µg/ml in 0.1 M $NaHCO_3$, pH 9.5) were applied to 96-well polystyrene microtitre
595 plates (Linbro/Titretek; ICN Biochemicals, Aurora, Ohio). The plates containing the *M.*
596 *hyopneumoniae* cells were centrifuged at 2000 × *g* for 10 min, while the plates containing
597 recombinant proteins were allowed to adsorb overnight at room temperature. The wells were
598 then blocked with 100 µl aliquots of PBS containing 2% (w/v) skim milk for 1 h at room
599 temperature. Biotinylated heparin (Sigma-Aldrich, St. Louis, Missouri) in PBS containing 1%
600 skim milk was next applied to the wells in 100 µl aliquots and incubated for 1.5 h at room
601 temperature. After 3 washes with 0.05% (v/v) Tween20 in PBS, bound biotinylated heparin was
602 detected using 100 µl aliquots of peroxidase conjugated streptavidin (Roche, Basel, Switzerland)
603 diluted 1:3000 with a 1 h incubation at room temperature. The wells were washed as above prior
604 to the addition of substrate solution (100 µl) containing 0.55 mg/ml 2,2'-azino-bis(3-
605 ethylebenzthiazoline-6-sulfonic acid) diammonium salt (ABTS; Sigma-Aldrich, St. Louis,
606 Missouri) in 0.1 M citrate, 0.2 M phosphate, pH 4.2, containing 0.03% (v/v) hydrogen peroxide.
607 The absorbance of the product formed was measured at 414 nm using a Multiskan Ascent
608 ELISA plate reader (Thermo Labsystems, Franklin, Massachusetts). In other experiments, a
609 competitive binding assay was used in which unlabeled glycosaminoglycans; heparin, fucoidan,

heparan sulfate, mucin, chondroitin sulphate A and chondroitin sulfate B (all from Sigma-Aldrich, St. Louis, Missouri) were pre-incubated with biotinylated heparin for 15 min before the addition of 100 µl aliquots of the mixture to coated and blocked wells. Control experiments showed that none of the P159 fragments could bind to streptavidin-peroxidase or the ABTS solution, establishing that the heparin binding is not an artifact of binding to a compound used in the detection system. Graph construction and non-linear regression with one-site binding and one-site competition analysis was performed using GraphPad Prism version 4 (GraphPad Software, San Diego, California).

A cell pellet of *E. coli* M15 [pREP4] cells (Qiagen, Alameda, California) containing the pQE-9 $F1_{P159}$-$F4_{P159}$ plasmids from a 300 ml culture were re-suspended in a solution of 50 mM DTT, 2% triton X-100, 1 mg/ml lysozyme. The suspension was subjected to sonication and then centrifuged at 16, 000 × g for 15 min at 10^{o}C and the supernatant was applied to a 7.5 ml heparin-agarose column (Sigma-Aldrich, St. Louis, Missouri) that had been pre-equilibrated with 0.01 M Tris-HCl (pH 7.6). The column was washed with 45 ml 0.01 M Tris-HCl (pH 7.6) and bound proteins eluted at a flow rate of 1 ml/min with a linear 0-0.5 M NaCl gradient in 0.01 M Tris-HCl (pH 7.6). The peak fractions (from the wash and elution's) at 280 nm absorbance were subjected to electrophoresis on 12% SDS-PAGE gels as described previously (Laemmli, 1970). After electrophoresis, proteins were electrophoretically transferred onto polyvinylidene difluoride membrane using a Hoefer Scientific TE Series Transphor Electrophoresis Unit (Hoefer, San Francisco, California) as described previously (Burnette, 1981). Immunoblotting experiments were performed using rabbit polyclonal antibodies raised separately to $F1_{P159}$-$F4_{P159}$. Peroxidase conjugated sheep anti-rabbit was used as the secondary antibody and detected using diaminobenzidine (DAB; Sigma-Aldrich, St. Louis, Missouri).

References

Adams, C., Pitzer, J., and Minion, F.C. (2005) *In vivo* expression analysis of the P97 and P102 paralog families of *Mycoplasma hyopneumoniae*. *Infect Immun* **73**: 7784-7787.

Aoki, K., Matsumoto, S., Hirayama, Y., Wada, T., Ozeki, Y., Niki, M., Domenech, P., Umemori, K., Yamamoto, S., Mineda, A., Matsumoto, M., and Kobayashi, K. (2004) Extracellular mycobacterial DNA-binding protein 1 participates in mycobacterium-lung epithelial cell interaction through hyaluronic acid. *J Biol Chem* **279**: 39798-39806.

Belloy, L., Vilei, E.M., Giacometti, M., and Frey, J. (2003) Characterization of LppS, an adhesin of *Mycoplasma conjunctivae*. *Microbiology* **149**: 185-193.

Bernfield, M., Gotte, M., Park, P.W., Reizes, O., Fitzgerald, M.L., Lincecum, J., and Zako, M. (1999) Functions of cell surface heparan sulfate proteoglycans. *Annu Rev Biochem* **68**: 729-777.

Blanchard, B., Vena, M.M., Cavalier, A., Le Lannic, J., Gouranton, J., and Kobisch, M. (1992) Electron microscopic observation of the respiratory tract of SPF piglets inoculated with *Mycoplasma hyopneumoniae*. *Vet Microbiol* **30**: 329-341.

Burnette, W.N. (1981) "Western blotting": electrophoretic transfer of proteins from sodium dodecyl sulfate--polyacrylamide gels to unmodified nitrocellulose and radiographic detection with antibody and radioiodinated protein A. *Anal Biochem* **112**: 195-203.

Cardin, A.D., and Weintraub, H.J. (1989) Molecular modeling of protein-glycosaminoglycan interactions. *Arteriosclerosis* **9**: 21-32.

Ciprian, A., Pijoan, C., Cruz, T., Camacho, J., Tortora, J., Colmenares, G., Lopez-Revilla, R., and de la Garza, M. (1988) *Mycoplasma hyopneumoniae* increases the susceptibility of pigs to experimental Pasteurella multocida pneumonia. *Can J Vet Res* **52**: 434-438.

Cordwell, S.J., Basseal, D.J., Bjellqvist, B., Shaw, D.C., and Humphery-Smith, I. (1997) Characterisation of basic proteins from Spiroplasma melliferum using novel immobilised pH gradients. *Electrophoresis* **18**: 1393-1398.

DeBey, M.C., and Ross, R.F. (1994) Ciliostasis and loss of cilia induced by *Mycoplasma hyopneumoniae* in porcine tracheal organ cultures. *Infect Immun* **62**: 5312-5318.

Djordjevic, S.P., Eamens, G.J., Romalis, L.F., and Saunders, M.M. (1994) An improved enzyme linked immunosorbent assay (ELISA) for the detection of porcine serum antibodies against *Mycoplasma hyopneumoniae*. *Vet Microbiol* **39**: 261-273.

Djordjevic, S.P., Cordwell, S.J., Djordjevic, M.A., Wilton, J., and Minion, F.C. (2004) Proteolytic processing of the *Mycoplasma hyopneumoniae* cilium adhesin. *Infect Immun* **72**: 2791-2802.

Dombek, P.E., Cue, D., Sedgewick, J., Lam, H., Ruschkowski, S., Finlay, B.B., and Cleary, P.P. (1999) High-frequency intracellular invasion of epithelial cells by serotype M1 group A streptococci: M1 protein-mediated invasion and cytoskeletal rearrangements. *Mol Microbiol* **31**: 859-870.

Duensing, T.D., Wing, J.S., and van Putten, J.P. (1999) Sulfated polysaccharide-directed recruitment of mammalian host proteins: a novel strategy in microbial pathogenesis. *Infect Immun* **67**: 4463-4468.

Friis, N.F. (1975) Some recommendations concerning primary isolation of *Mycoplasma suipneumoniae* and *Mycoplasma flocculare* a survey. *Nord Vet Med* **27**: 337-339.

680 Futo, S., Seto, Y., Mitsuse, S., Mori, Y., Suzuki, T., and Kawai, K. (1995) Molecular cloning of
681 a 46-kilodalton surface antigen (P46) gene from *Mycoplasma hyopneumoniae*: direct
682 evidence of CGG codon usage for arginine. *J Bacteriol* **177**: 1915-1917.
683 Hsu, T., Artiushin, S., and Minion, F.C. (1997) Cloning and functional analysis of the P97 swine
684 cilium adhesin gene of *Mycoplasma hyopneumoniae*. *J Bacteriol* **179**: 1317-1323.
685 Hsu, T., and Minion, F.C. (1998) Identification of the cilium binding epitope of the *Mycoplasma*
686 *hyopneumoniae* P97 adhesin. *Infect Immun* **66**: 4762-4766.
687 Jackson, R.L., Busch, S.J., and Cardin, A.D. (1991) Glycosaminoglycans: molecular properties,
688 protein interactions, and role in physiological processes. *Physiol Rev* **71**: 481-539.
689 Jenkins, C., Wilton, J., Minion, F., Falconer, L., Walker, M., and Djordjevic, S. (2006) Two
690 Domains within the *Mycoplasma hyopneumoniae* Cilium Adhesin Bind Heparin. *Infect*
691 *Immun* **74**. In Press.
692 Kim, M.F., Heidari, M.B., Stull, S.J., McIntosh, M.A., and Wise, K.S. (1990) Identification and
693 mapping of an immunogenic region of *Mycoplasma hyopneumoniae* p65 surface
694 lipoprotein expressed in Escherichia coli from a cloned genomic fragment. *Infect Immun*
695 **58**: 2637-2643.
696 Kobisch, M., Blanchard, B., and Le Potier, M.F. (1993) *Mycoplasma hyopneumoniae* infection
697 in pigs: duration of the disease and resistance to reinfection. *Vet Res* **24**: 67-77.
698 Laemmli, U.K. (1970) Cleavage of structural proteins during the assembly of the head of
699 bacteriophage T4. *Nature* **227**: 680-685.
700 Livingston, C.W., Jr., Stair, E.L., Underdahl, N.R., and Mebus, C.A. (1972) Pathogenesis of
701 mycoplasmal pneumonia in swine. *Am J Vet Res* **33**: 2249-2258.
702 Mebus, C.A., and Underdahl, N.R. (1977) Scanning electron microscopy of trachea and bronchi
703 from gnotobiotic pigs inoculated with *Mycoplasma hyopneumoniae*. *Am J Vet Res* **38**:
704 1249-1254.
705 Menozzi, F.D., Pethe, K., Bifani, P., Soncin, F., Brennan, M.J., and Locht, C. (2002) Enhanced
706 bacterial virulence through exploitation of host glycosaminoglycans. *Mol Microbiol* **43**:
707 1379-1386.
708 Minion, F.C., Adams, C., and Hsu, T. (2000) R1 region of P97 mediates adherence of
709 *Mycoplasma hyopneumoniae* to swine cilia. *Infect Immun* **68**: 3056-3060.
710 Minion, F.C. (2002) Molecular pathogenesis of mycoplasma animal respiratory pathogens. *Front*
711 *Biosci* **7**: d1410-1422.
712 Minion, F.C., Lefkowitz, E.J., Madsen, M.L., Cleary, B.J., Swartzell, S.M., and Mahairas, G.G.
713 (2004) The genome sequence of *Mycoplasma hyopneumoniae* strain 232, the agent of
714 swine mycoplasmosis. *J Bacteriol* **186**: 7123-7133.
715 Molinari, G., Talay, S.R., Valentin-Weigand, P., Rohde, M., and Chhatwal, G.S. (1997) The
716 fibronectin-binding protein of *Streptococcus pyogenes*, SfbI, is involved in the
717 internalization of group A streptococci by epithelial cells. *Infect Immun* **65**: 1357-1363.
718 Notarnicola, S.M., McIntosh, M.A., and Wise, K.S. (1990) Multiple translational products from
719 a *Mycoplasma hyorhinis* gene expressed in *Escherichia coli*. *J Bacteriol* **172**: 2986-2995.
720 Nouwens, A.S., Cordwell, S.J., Larsen, M.R., Molloy, M.P., Gillings, M., Willcox, M.D., and
721 Walsh, B.J. (2000) Complementing genomics with proteomics: the membrane
722 subproteome of Pseudomonas aeruginosa PAO1. *Electrophoresis* **21**: 3797-3809.
723 Pankhurst, G.J., Bennett, C.A., and Easterbrook-Smith, S.B. (1998) Characterization of the
724 heparin-binding properties of human clusterin. *Biochemistry* **37**: 4823-4830.
725 Patankar, M.S., Oehninger, S., Barnett, T., Williams, R.L., and Clark, G.F. (1993) A revised
726 structure for fucoidan may explain some of its biological activities. *J Biol Chem* **268**:
727 21770-21776.
728 Patti, J.M., Allen, B.L., McGavin, M.J., and Hook, M. (1994) MSCRAMM-mediated adherence
729 of microorganisms to host tissues. *Annu Rev Microbiol* **48**: 585-617.

Pethe, K., Aumercier, M., Fort, E., Gatot, C., Locht, C., and Menozzi, F.D. (2000) Characterization of the heparin-binding site of the mycobacterial heparin-binding hemagglutinin adhesin. *J Biol Chem* **275**: 14273-14280.

Sambrook, J., Fritsch, E.F., and Maniatis, T. (1989) *Molecular Cloning: A Laboratory Manual.* Cold Spring Harbour, NY: Cold Spring Harbour Laboratory Press.

Scarman, A.L., Chin, J.C., Eamens, G.J., Delaney, S.F., and Djordjevic, S.P. (1997) Identification of novel species-specific antigens of *Mycoplasma hyopneumoniae* by preparative SDS-PAGE ELISA profiling. *Microbiology* **143**: 663-673.

Tajima, M., and Yagihashi, T. (1982) Interaction of *Mycoplasma hyopneumoniae* with the porcine respiratory epithelium as observed by electron microscopy. *Infect Immun* **37**: 1162-1169.

Thacker, E.L., Thacker, B.J., Young, T.F., and Halbur, P.G. (2000) Effect of vaccination on the potentiation of porcine reproductive and respiratory syndrome virus (PRRSV)-induced pneumonia by *Mycoplasma hyopneumoniae*. *Vaccine* **18**: 1244-1252.

Vasconcelos, A.T., Ferreira, H.B., Bizarro, C.V., Bonatto, S.L., Carvalho, M.O., Pinto, P.M., *et al*., (2005) Swine and poultry pathogens: the complete genome sequences of two strains of *Mycoplasma hyopneumoniae* and a strain of *Mycoplasma synoviae*. *J Bacteriol* **187**: 5568-5577.

Vicca, J., Stakenborg, T., Maes, D., Butaye, P., Peeters, J., de Kruif, A., and Haesebrouck, F. (2003) Evaluation of virulence of *Mycoplasma hyopneumoniae* field isolates. *Vet Microbiol* **97**: 177-190.

Wadstrom, T., and Ljungh, A. (1999) Glycosaminoglycan-binding microbial proteins in tissue adhesion and invasion: key events in microbial pathogenicity. *J Med Microbiol* **48**: 223-233.

Wilton, J.L., Scarman, A.L., Walker, M.J., and Djordjevic, S.P. (1998) Reiterated repeat region variability in the ciliary adhesin gene of Mycoplasma hyopneumoniae. *Microbiology* **144**: 1931-1943.

Zhang, Q., Young, T.F., and Ross, R.F. (1994) Microtiter plate adherence assay and receptor analogs for *Mycoplasma hyopneumoniae*. *Infect Immun* **62**: 1616-1622.

Zhang, Q., Young, T.F., and Ross, R.F. (1995) Identification and characterization of a *Mycoplasma hyopneumoniae* adhesin. *Infect Immun* **63**: 1013-1019.

Zielinski, G.C., Young, T., Ross, R.F., and Rosenbusch, R.F. (1990) Adherence of *Mycoplasma hyopneumoniae* to cell monolayers. *Am J Vet Res* **51**: 339-343.

Table 1. Sequences of primers used in this study.

Designation	Sequence	Length (bp)	Target
F1 (F)	GGGTCGACAATTCAGCGCTTAGATCC	26	*p159* F1 F primer
F2 (F)	GGGTCGACCAAACAAGTCAAAGCTCAGAA	29	*p159* F2 F primer
F3 (F)	GGGTCGACAAGACCTCAGAGGCAAGTAAT	29	*p159* F3 F primer
F4 (F)	GGGTCGACCACAAAATAACAACTTTCCAA	29	*p159* F4 F primer
F1 (R)	GGCTGCAGTCACCCTTTTTGATCTGTTGA	29	*p159* F1 R primer
F2 (R)	GGCTGCAGTCATGGTGCTGTCTCTGGTGA	29	*p159* F2 R primer
F3 (R)	GGCTGCAGTCAATCTTTTTCTTGGTCATG	29	*p159* F3 R primer
F4 (R)	GGCTGCAGTCAATATTGATCCATAAAGGC	29	*p159* F4 R primer
713	GGGGGATCCATGAAGAAACAAATTCGCAAC	30	*p159* F primer
714	GGGGGATCCTTATTAAGAATAATTCTTAAAATATTGATCC	40	*p159* R primer
p110W_1014F	CAGAAATTATCAATTGGTAGATGGTATAATGCGCCCCAAAG	41	*p159* SDM primer
p110W_1014R	CTTTGGGGCGCATTATACCATCTACCAATTGATAATTTCTG	41	*p159* SDM primer
p110W_1213F	GAAAACCTTAAATTAGTCTGGAAACTAATCGGGGC	35	*p159* SDM primer
p110W_1213R	GCCCCGATTAGTTTCCAGACTAATTTAAGGTTTTC	35	*p159* SDM primer
p110W_1293F	CTTGGTCAAACTTGGTTAATGGAAATAAG	29	*p159* SDM primer
p110W_1293R	CTTATTTCCATTAACCAAGTTTGACCAAG	29	*p159* SDM primer
p110W_1323F	GCAAACTAAAAGTTTGGAAATCCGAAATTAAG	32	*p159* SDM primer
p110W_1323R	CTTAATTTCGGATTTCCAAACTTTTAGTTTGC	32	*p159* SDM primer
p110W_1342F	CCAAAACCAGGATACAAACTGGGAAACCGAGCTAGCTTC	39	*p159* SDM primer
p110W_1342R	GAAGCTAGCTCGGTTTCCCAGTTTGTATCCTGGTTTTGG	39	*p159* SDM primer
p110W_462F	CAGGAAGTAATTTGGAGTTTTTCAAGG	27	*p159* SDM primer
p110W_462R	CCTTGAAAAACTCCAAATTACTTCCTG	27	*p159* SDM primer
p110W_623F	CTAAAAATTCATGGTTGGAATTATAGAACAC	31	*p159* SDM primer
p110W_623R	GTGTTCTATAATTCCAACCATGAATTTTTAG	31	*p159* SDM primer
p110W_73F	GCTTAAAAGAAAACTGGAGTAAAATATCAGCTGG	34	*p159* SDM primer
p110W_73R	CCAGCTGATATTTTACTCCAGTTTTCTTTTAAGC	34	*p159* SDM primer
p110W_759F	GCTTATGAATTAAAGGGTTGGACTTATCCAATTG	34	*p159* SDM primer
p110W_759R	CAATTGGATAAGTCCAACCCTTTAATTCATAAGC	34	*p159* SDM primer

Restriction sites for *Sal*I in the forward (F) primers and *Pst*I in the reverse (R) primers used for cloning the *p159* fragments $F1_{P159}$-$F4_{P159}$ into pQE-9 are underlined. SDM refers to site-directed mutagenesis.

798

799

800 **Figure legends**

801 **Fig. 1.** 2-DGE and peptide mass fingerprint analysis of P159. (A) 2-D gel (8-18%
802 polyacrylamide gradient) of *M. hyopneumoniae* strain 232 whole cell lysate. Proteins were
803 resolved using a pH 6-11 first dimension isoelectric focusing strip prior to SDS-PAGE. P159
804 cleavage fragments P27, P52 and P110 identified by peptide mass mapping are indicated. Spot
805 trains (commonly observed for proteins resolved by 2-DGE electrophoresis) may be due to bona
806 fide posttranslational modifications that evoke a pI shift (e.g. phosphorylation) or are artifactual
807 arising by non-enzymatic deamidation of Asn to Asp. (B) Peptide mass mapping was performed
808 using MALDI-TOF (MS) analysis on tryptic digests of P159 proteins boxed in panel A. The N-
809 terminal sequence of P27 as determined by Edman degradation is underlined. The predicted
810 transmembrane region is double underlined. (C) Diagrammatic representation of the P159
811 molecule depicting P27, P110 and P52. The four P159 recombinant fragments ($F1_{P159}$-$F4_{P159}$)
812 constructed for this study are also shown. The cleavage site between P27 and P110 is predicted
813 to occur between amino acids 220-302 whilst cleavage between P110 and P52 is predicted to
814 occur between amino acids 842-977.

815

816

817 **Fig. 2.** Immunoblot analyses using $F1_{P159}$, $F2_{P159}$, $F3_{P159}$, and $F4_{P159}$ antisera. Panels A-D show
818 whole cell protein extracts of *M. hyopneumoniae* strain 232 (lane 1) and a sample of purified
819 $F1_{P159}$, $F2_{P159}$, $F3_{P159}$, and $F4_{P159}$ proteins (lane 2, panels A-D respectively) reacted with anti-
820 $F1_{P159}$ (panel A), anti-$F2_{P159}$ (panel B), anti-$F3_{P159}$ (panel C), and anti-$F4_{P159}$ sera (panel D).
821 Antisera were diluted 1/100. All preparations were boiled for 5 min in Laemmli buffer. Black
822 arrowheads indicate the position of recombinant proteins $F1_{P159}$-$F4_{P159}$. White arrowheads

823 indicate the position of dominant cleavage fragments recognised by antisera in whole cell lysates
824 of *M. hyopneumoniae*. The asterix (*) identifies a multimeric form of recombinant protein
825 $F4_{P159}$. An immunoblot containing comparable amounts of whole cell lysates of *M.*
826 *hyopneumoniae* strain 232 harvested at different times during the growth cycle reacted with a
827 pool of anti $F1_{P159}$-$F4_{P159}$ sera is shown in panel E. Lanes 1-9 correspond to *M. hyopneumoniae*
828 cultures harvested at 8, 16, 24, 28, 32, 40, 48, 56 and 72 hours post inoculation respectively. An
829 immunoblot containing comparable amounts of whole cell lysates of various *M. hyopneumoniae*
830 strains reacted with a pool of anti $F1_{P159}$-$F4_{P159}$ sera is shown in panel F. Lane 1-5 were loaded
831 with lysates of strains 232, J, SUE, C1735/2, and Beaufort respectively.
832
833 **Fig. 3.** Localization of P159 cleavage products on the surface of *M. hyopneumoniae* strain 232.
834 Panel A shows an immunoblot of whole cell preparations of freshly cultured *M. hyopneumoniae*
835 strain 232 cells exposed to different concentrations of trypsin ranging from 0, 0.1, 0.5, 1, 3, 5,
836 10, 50 and 150 μg/ml for 15 minutes (lanes 1-9 respectively) reacted with a pool of rabbit anti-
837 $F1_{P159}$-$F4_{P159}$ sera. Panels B-E show electron micrographs of intact, freshly cultured *M.*
838 *hyopneumoniae* strain 232 cells labeled with pre-immune, control sera collected prior to
839 immunization with recombinant proteins $F2_{P159}$ and $F4_{P159}$ (panels B and D respectively) or
840 hyper-immune rabbit anti-$F2_{P159}$ and anti-$F4_{P159}$ sera (panel C and E respectively). Colloidal
841 gold-conjugated anti-rabbit Ig (15 nm particles) was used to detect P159 cleavage fragments
842 recognized by these sera. Cells were stained with 2% aqueous uranyl acetate. Arrows indicate
843 gold particles. Bars = 500 nm.
844
845 **Fig. 4.** Binding of biotinylated heparin to *M. hyopneumoniae* strain 232. Binding of biotinylated
846 heparin to the surface of *M. hyopneumoniae* strain 232 is shown in panel A. Increasing
847 concentrations of biotinylated heparin were added to 96-well microtitre plates coated with *M.*

hyopneumoniae strain 232. Figures shown are means ± SEM of triplicate determinations, indicated by error bars. A ligand blot containing *M. hyopneumoniae* strain 232 whole cell lysate probed with biotinylated heparin is shown in panel B.

Fig. 5. Binding of recombinant P159 fragments ($F1_{P159}$-$F4_{P159}$) to biotinylated heparin. Increasing concentrations of biotinylated heparin were added to 96-well microtitre plates coated with 5 μg/ml of each of the four P159 fragments. □ represents the total binding and Δ represents non-specific binding measured by mixing the biotinylated heparin with a 50-fold excess (2.4 mg/ml) of non-biotin labeled heparin prior to incubation with the recombinant P159 fragments. The specific binding curve, represented by the symbol ○, was obtained by subtracting non-specific binding from the total binding values. Figures shown are means ± SEM of triplicate determinations, indicated by error bars. Controls with specific antisera show that each protein was successfully coated to the ELISA plate.

Fig. 6. Inhibition studies with various glycosaminoglycans. Different glycosaminoglycans were examined for their ability to inhibit the binding of recombinant P159 fragments to biotinylated heparin. Panel A shows how unlabeled heparin affects the ability of $F1_{P159}$ (□), $F2_{P159}$ (Δ), $F3_{P159}$ (○) and $F4_{P159}$ (◊) to bind biotinylated heparin. Panels B and C show how unlabeled fucoidan ■, heparan sulfate ▲, chondroitin sulfate A ●, and chondroitin sulfate B ♦ affect the ability of $F3_{P159}$ and $F4_{P159}$ to bind biotinylated heparin respectively. Inset are inhibition curves showing an expansion of the optimal inhibition range of 0-600 μg/ml. In these experiments, varying concentrations (0-40 times the saturating concentration of 60 μg/ml) of glycosaminoglycan inhibitors were each pre-incubated with biotinylated heparin (60 μg/ml). Error bars represents mean values ± SEM from triplicate experiments.

Fig. 7. Scanning electron micrographs depicting the interaction of *M. hyopneumoniae* with PK15 cells. Panel A shows *M. hyopneumoniae* interacting with PK15 cells. Panel B shows the inhibition of *M. hyopneumoniae* adherence due to the presence of $F4_{P159}$ protein (1 μg). Adhering *M. hyopneumoniae* cells are indicated by an arrow. Panel C shows the inhibition of adherence due to the presence of heparin (500 μg/ml). Scale bars are given at the bottom of each image.

Fig. 8. Double immunofluorescence microscopy of PK15 cells exposed to latex beads coated with recombinant P159 proteins. Beads determined to reside intracellularly are identified with white arrows. Panel A shows PK15 cells incubated with $F1_{P159}$ -coated latex beads after 22 h incubation. These images are indistinguishable from control images of PK15 cells exposed to naïve latex beads and show that $F1_{P159}$ does not play a direct role in adherence. Panel B shows $F2_{P159}$- coated latex beads after 7 h of incubation adhering to the surface of (yellow/green) and penetrating into (orange/red) PK15 cells. Panel C shows a similar image as depicted in B except the nucleus of the PK15 cells were stained with Hoechst stain. Panel D depicts the same image as panel C but with a different exposure time showing the extracellular (yellow/green) beads and the intracellular (orange/red) beads. Panel E shows $F3_{P159}$-coated beads interacting with a cluster of PK15 cells after 4 h of incubation. Panel F depicts $F4_{P159}$-coated beads interacting with PK15 cells after 7 h incubation. Beads were identified on the surface (yellow/green beads) and within (orange/red beads) PK15 cells.

Fig. 9. Scanning electron micrographs depicting the interaction of latex beads separately coated with recombinant P159 fragments $F2_{P159}$ and $F4_{P159}$ with PK15 cells. Panels A and B depict $F2_{P159}$- and $F4_{P159}$- coated latex beads adhering to and residing within PK15 cells respectively. Panel C represents an enlargement of the area (marked by an arrow) in panel A showing an

898 $F2_{P159}$- coated bead adhering to and another within a PK15 cell 2 h after incubation. Similarly,
899 panel D represents the arrow marked area in panel B showing a $F4_{P159}$- coated bead adhering to
900 and another within a PK15 cell 2 h after incubation. Panels E and F depict $F4_{P159}$- coated latex
901 beads adhering to and residing inside PK15 cells 2 and 4 h after incubation respectively. The
902 scale bars are given at the bottom of each image.
903
904 **Fig. 10.** Inhibition of binding of $F2_{P159}$ and $F4_{P159}$- coated latex beads to PK15 cells. $F2_{P159}$-
905 coated latex beads pre-incubated with $F2_{P159}$ bound poorly to PK15 cells (panel A). $F4_{P159}$-
906 coated latex beads pre-incubated with $F4_{P159}$ protein bound poorly to PK15 cells (panel B). An
907 adherent bead is highlighted by an arrow. $F4_{P159}$- coated latex beads pre-incubated with heparin
908 bound poorly to PK15 cells (panel C). Scale bars represent 10 μm. Panel D summarises data
909 derived from three individual assays (20 cells counted per assay). Error bars represent the
910 standard deviation. Latex beads were pre-incubated with a saturating concentration of heparin
911 (500 μg/ml) or protein (1 μg) for 1h before addition to the PK15 cells. Numbers of adhering
912 (extracellular) and invasive (intracellular) beads were quantified by double immunofluorescence
913 analysis.
914
915
916
917
918
919
920
921
922
923
924
925
926
927
928
929
930
931

Acknowledgements

The skillful technical assistance of K. Abul, A. Collins, L. Falconer, N. Janze, I. Schleicher and R. Schmidt are acknowledged. *M. hyopneumoniae* J strain (ATCC 27715) was kindly supplied by P. Valentin-Weigand, University of Veterinary Medicine Hannover, Germany. We are grateful for the efforts of Dr. Graeme Eamens for proofreading the manuscript. T.A. Burnett is the recipient of an Australian Postgraduate Award. This work was partly supported by a grant from the McGarvie Smith Trust and an Australian Research Council Linkage Grant (LP0455306).

Fig. 1

A

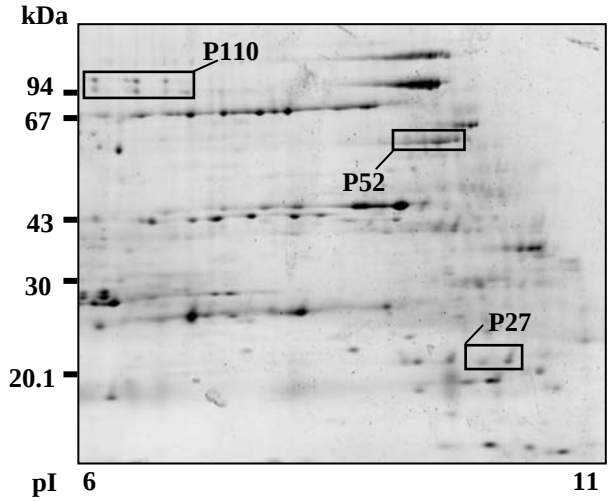

B

MKKQIRNKAIIVLAGLSFIGITAGVGLAVQNSALRSSYLNQFKNDKSATELLSPINDTELSKIISNFSLK**E**
NWSKISAGQAFELHKNPLYAFK**LTDAIDFSKIDKKFAHLFFNVQVNDNTKVEGNSIR**NLTVFVFDAITKK**E** **P27**
VATRAFHTSLSGFSSVAK**EDFIENFVAESSTYELDKDQLKK**NFATEIVLPSAFSIKFQDVLLTHLRKTSPE
SFQETK**TIQVRALTNSITEFQQQQQEGGSGGSGTSGGSSGGSSSGSTDQKGQTSQSSEKESKSEKEKGKDQ
QSTQGSEQKQDQKQQKPK**EAEKPAQEKPAQEKPAETPK**VKAPVIEPVKKLVFENEKLNQALLETLKDFGGL**
KLLAASGLQGLLPNEYTLLPVSSDK**SLIK**LDIDDQAGTASIHLK**LLDKNKKEKNLILPINGLASIGAIK**DK
VFSQIFRNQNAYLTIRPQINEYLR**KNPRKK**IQEVIWSFSREKFDQLRGQNEVEKFLEELYNPTQTSQSPQK
SKSSDSAKNNVATIQASPETAPKTTTTNSNTQSSSTSTNNQSSNGSQQMASPQTESSLSTAKTSEASNSSE **P110**
ESSSETKGTKEQANSETNPMGKSQAKPEAKPEEKQINLEDQAK**TELKEILK**IHGWNYRTLLKDQNQKVILP
DNINFWFDLR**NKR**SSYENYKLEFDLVK**K**TGQIQAGDVIDANKIR**LNLKISPLANLKLEVDSKNK**QYIDAGQ
IGDYVEFDKQGK**KLVEQGKSLDLK**VGASAANSIFSPEIRYSAYELK**GWTYPIDIDIK**GNPIQQELEK**LVGN**
FHKVGINKNNQYQIYSTDIDKIFAQAKLDKYFELSQEEK**QASKKYLQEK**LNPISEITIVK**LPPKEEVLPPL**
EEEKKPEQDQKAQEKQEDKQNQKQQEKQEDKKEQDQQKHSQSPDQKTETQTHDQEKDKQTSSETSPSNTNE
SSGTQNTAQNSQTNQANSGQGQSQQAASSSTSYQTHKITTFQDDQKDQTNEQTEKEIEPEKLAFGDYLVKY
LDIFETFK**VGPDQKLSIGR**WYNAPQRTYNVIFRVLDKENIQVAASLFQLHGISATNIALEK**SLR**YAPDIFL
DGTSGLEYKQDTGDKPYLQGRQFVSAINSINNTK**SSYRVHK**LFDNLPLSEESSQGLR**LK**SSLVYDYQKNDP
YTFQASK**EALRKTALTKGVLYLAFKPEQILGIKGSKTAPGRNYK**LLSTTNVHFKSLYGLSNLELVK**TKYQE**
NLKLVWKLIGAKPVNDDKILPPQVADLPR**HRSTEIILLEDSKPGASSSPQTK**ENSQNKEAETFNLDIRQTK
PNQIEPLEHYLGQTWLMEIRIDDESATITIIPEQQEREDSK**LKVWKSEIKIKDK**NKYQNQDTNWETELASV
LGRGFDYGQIGDTTPQASNPQDR**VGMTFK**GFAVFKGDK**LLNDKARLNVRKAFMDQYFKNYS**

C

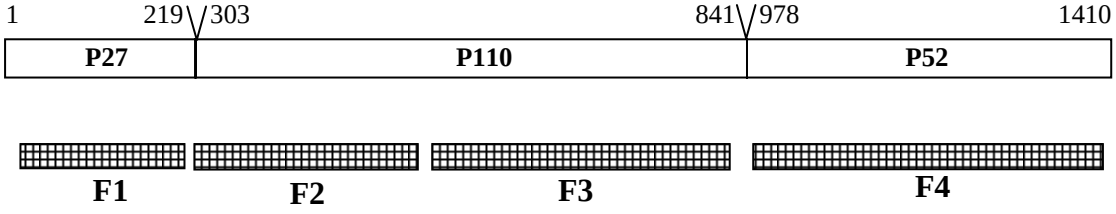

Fig. 2

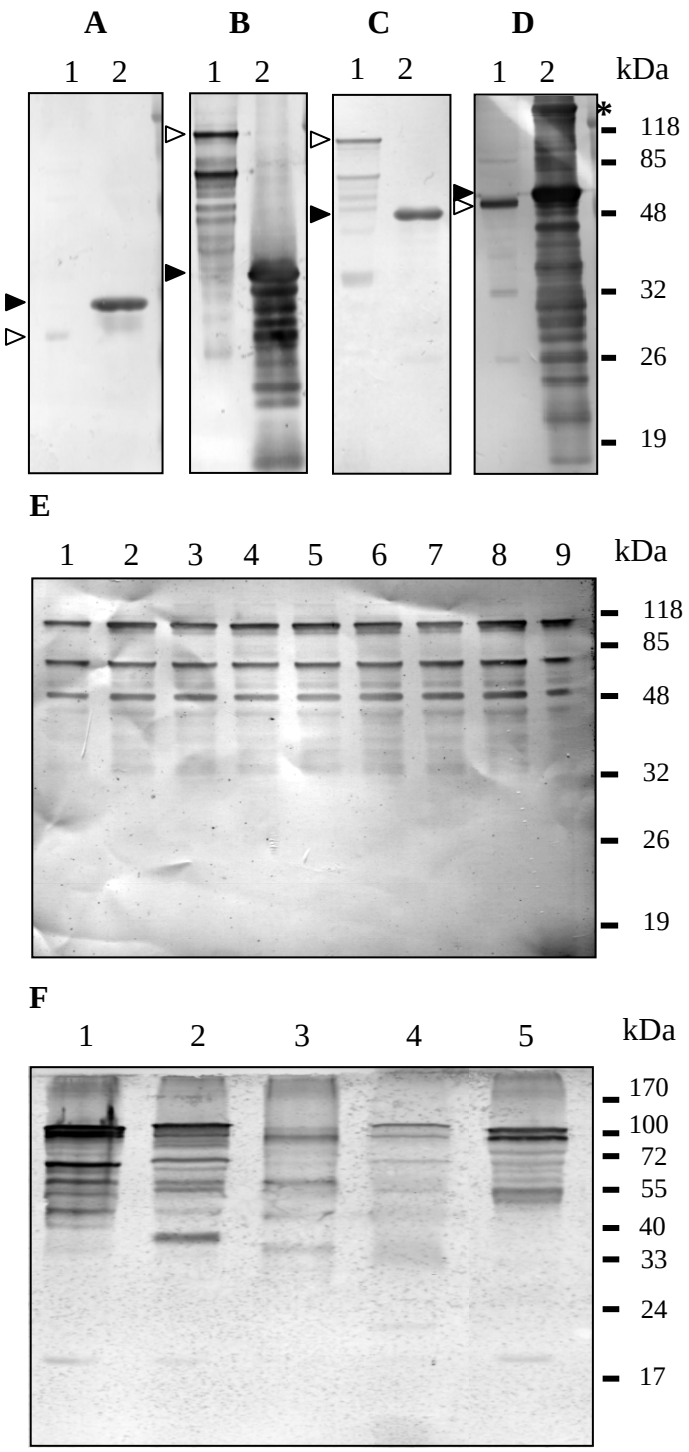
A
B
C
D
1 2
1 2
1 2
1 2
kDa
*
118
85
48
32
26
19
E
1 2 3 4 5 6 7 8 9
kDa
118
85
48
32
26
19
F
1 2 3 4 5
kDa
170
100
72
55
40
33
24
17

Fig. 3

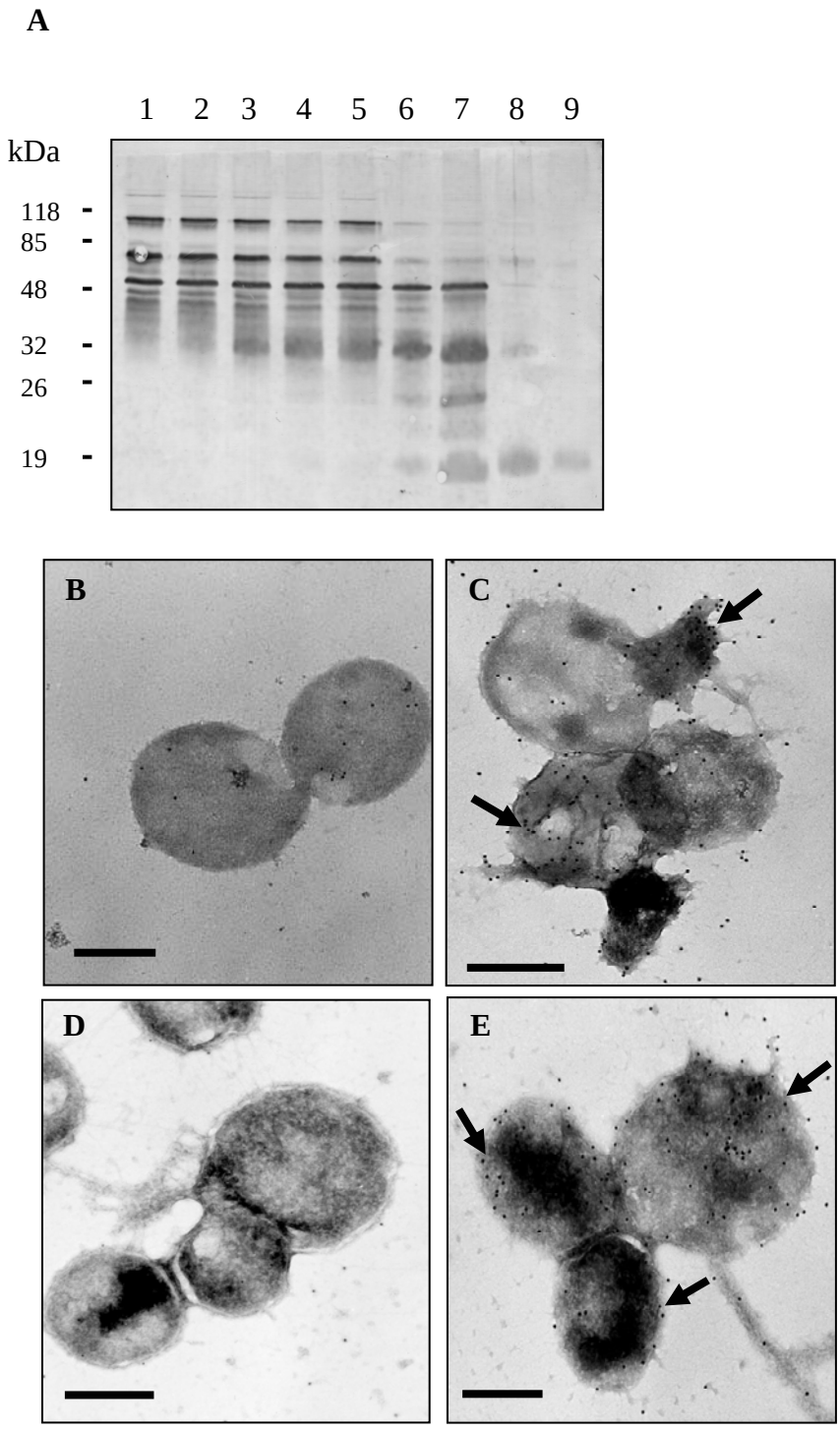

87 **Fig. 4**

88

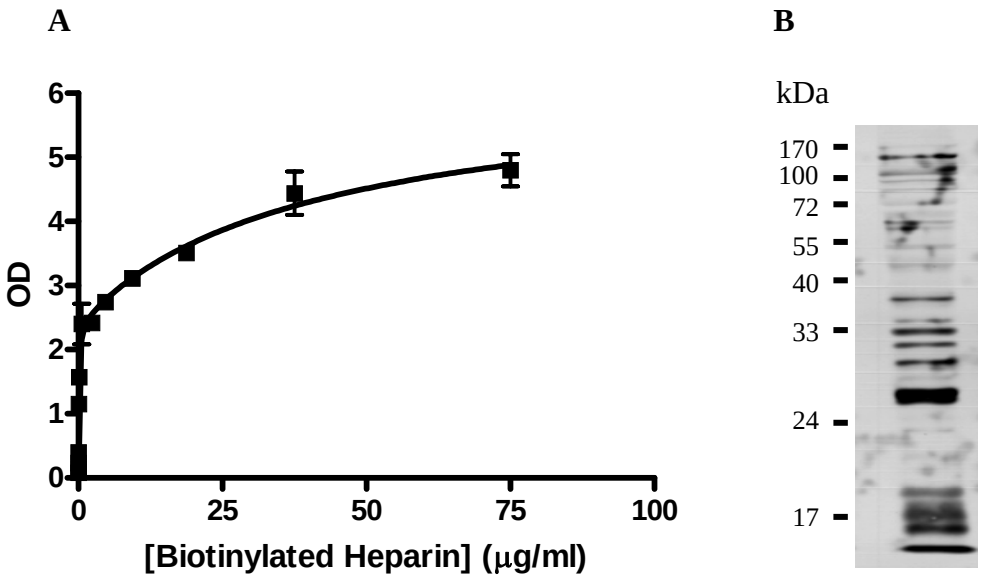

89

90

Fig. 5

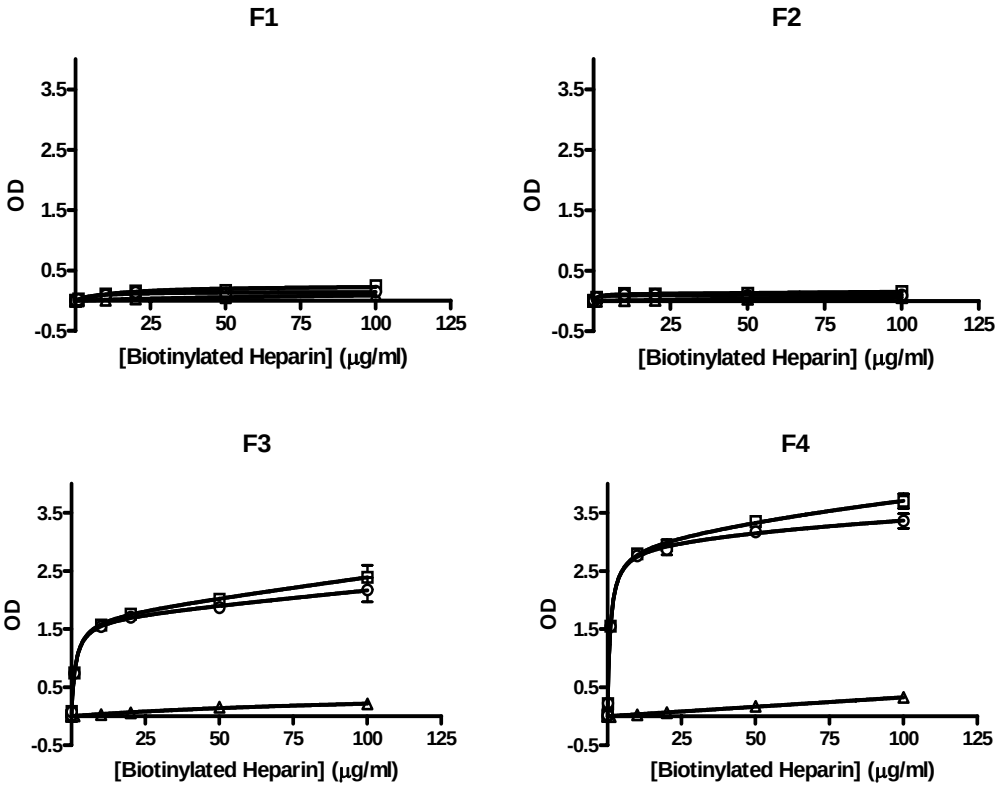
F1
F2
F3
F4
OD
3.5
2.5
1.5
0.5
-0.5
25
50
75
100
125
[Biotinylated Heparin] (µg/ml)

Fig. 6

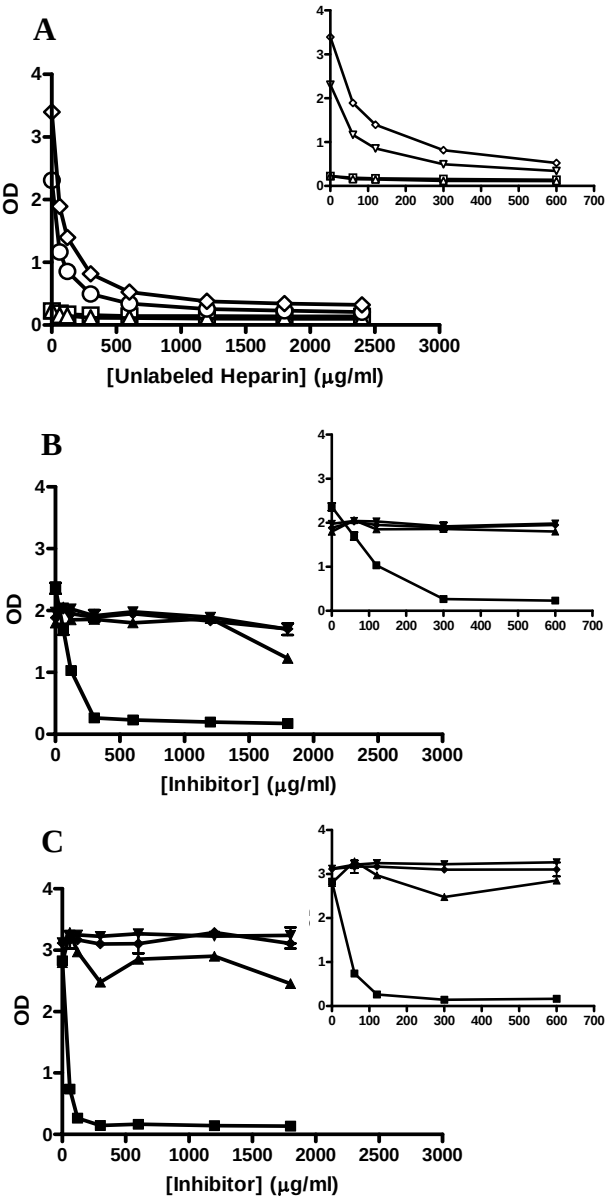
A
OD
[Unlabeled Heparin] (μg/ml)
B
OD
[Inhibitor] (μg/ml)
C
OD
[Inhibitor] (μg/ml)

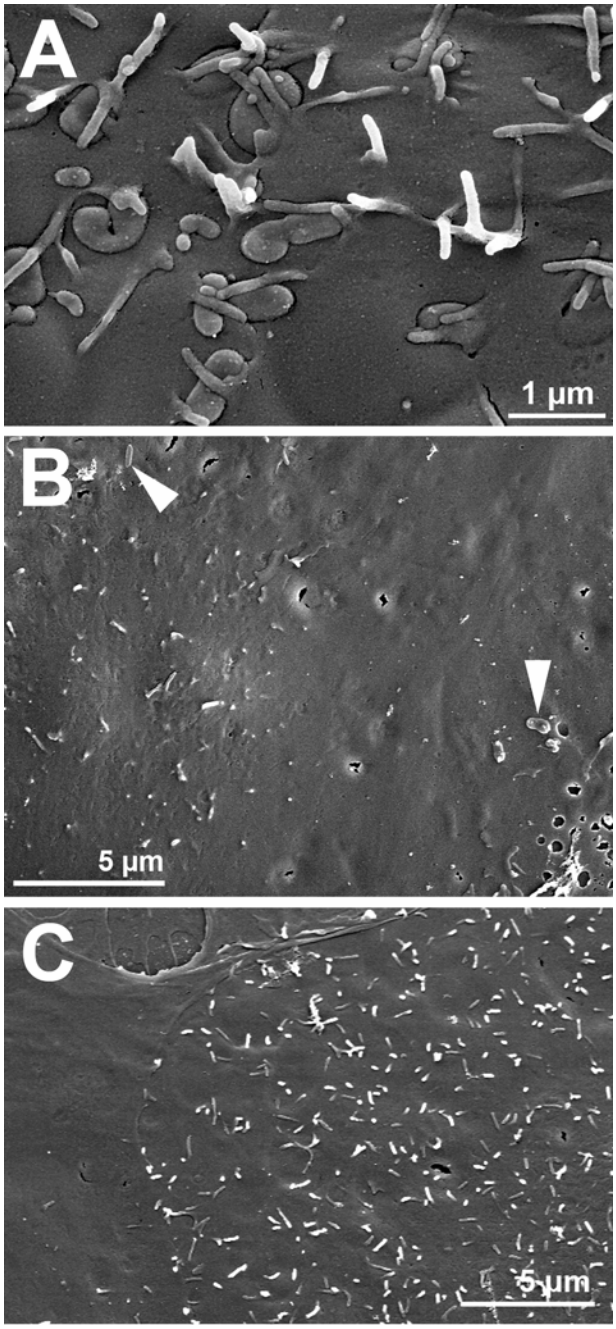
A
1 µm
B
5 µm
C
5 µm

Fig. 8.

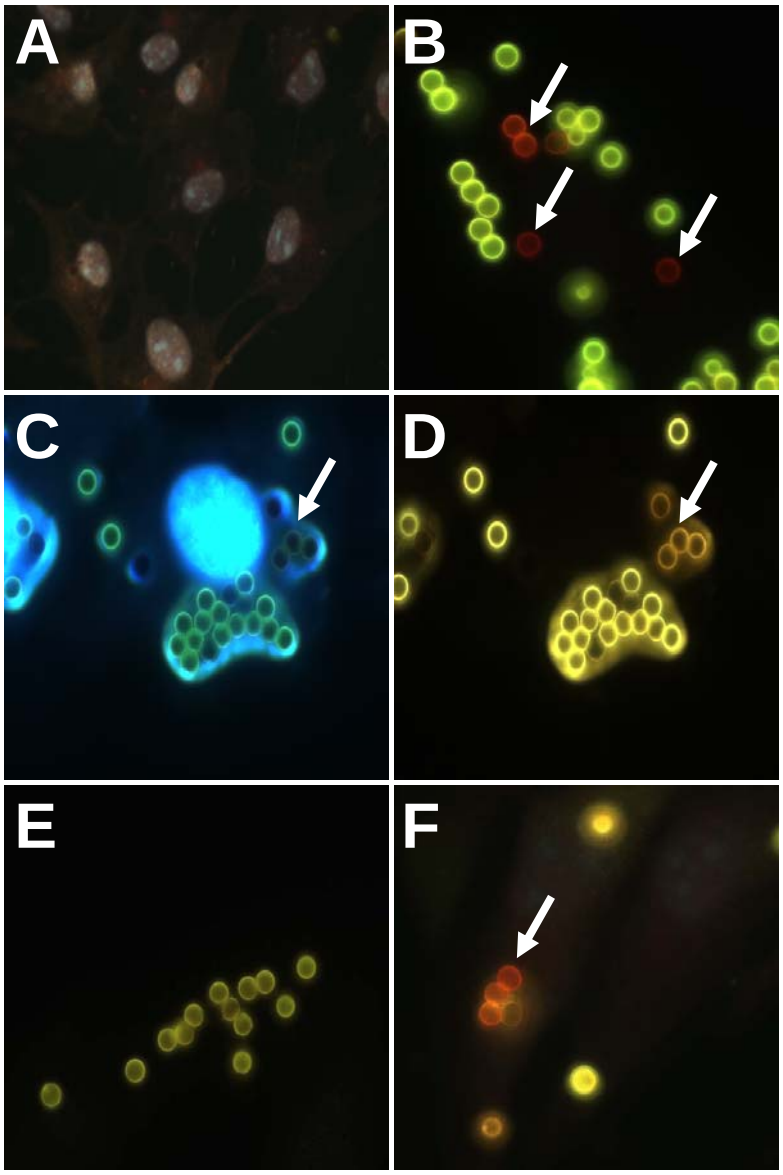

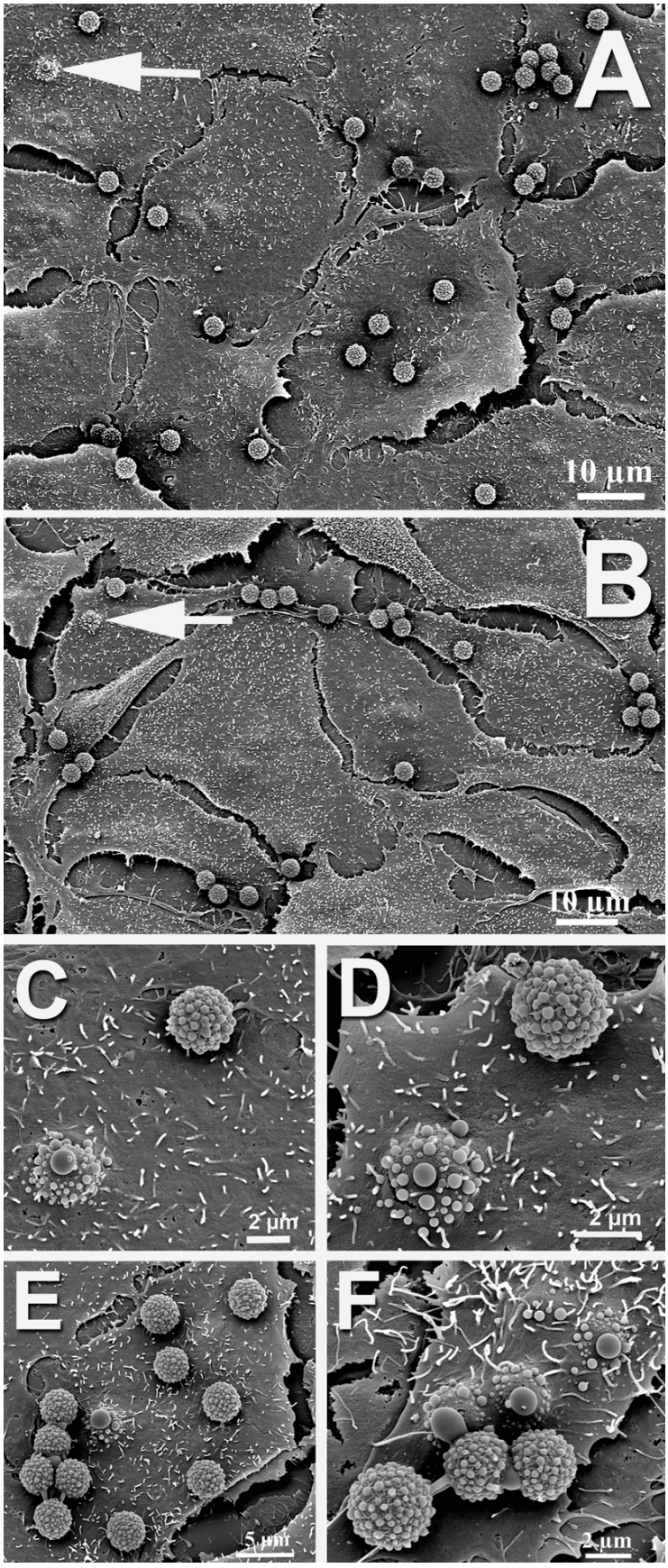

1

1

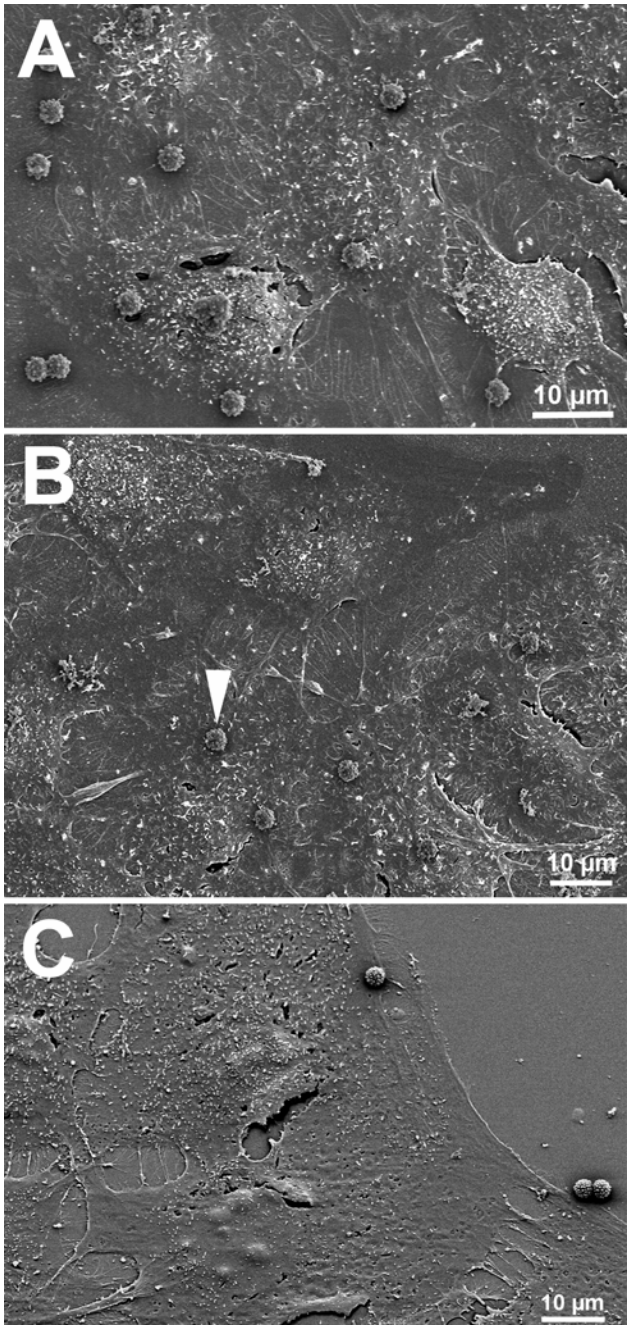
A
10 µm
B
10 µm
C
10 µm

2

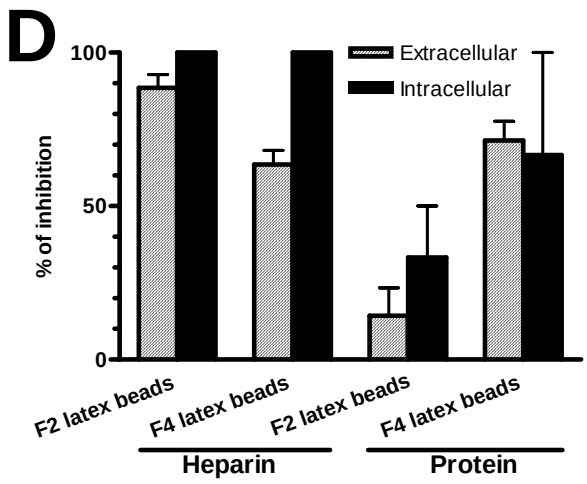
D
100
50
0
% of inhibition
Extracellular
Intracellular
F2 latex beads
F4 latex beads
F2 latex beads
F4 latex beads
Heparin
Protein